Digital Comprehensive Summaries of Uppsala Dissertations
from the Faculty of Science and Technology 2307

Analytical developments and applications of ambient mass spectrometry imaging

Visualizing challenging analytes and understanding chemical mechanisms of ischemic stroke

LEONIDAS MAVROUDAKIS

ACTA UNIVERSITATIS
UPSALIENSIS
2023

ISSN 1651-6214
ISBN 978-91-513-1897-4
urn:nbn:se:uu:diva-511811

UPPSALA
UNIVERSITET

Dissertation presented at Uppsala University to be publicly examined in Room B42, BMC, Husargatan 3, Uppsala, Friday, 3 November 2023 at 09:15 for the degree of Doctor of Philosophy. The examination will be conducted in English. Faculty examiner: Professor Malcolm Clench (Sheffield Hallam University, UK).

Abstract

Mavroudakis, L. 2023. Analytical developments and applications of ambient mass spectrometry imaging. Visualizing challenging analytes and understanding chemical mechanisms of ischemic stroke. *Digital Comprehensive Summaries of Uppsala Dissertations from the Faculty of Science and Technology* 2307. 85 pp. Uppsala: Acta Universitatis Upsaliensis. ISBN 978-91-513-1897-4.

Bioanalytical methods that provide spatial information on molecular distributions are important for deep understanding of chemical mechanisms in health and disease. For instance, the localized action of drugs and metabolites can provide valuable information on metabolism in specific cellular regions, which would not be possible with bulk analysis. Mass spectrometry imaging (MSI) is a powerful tool for realizing molecular distributions directly from the surface of biological samples e.g., tissue sections. Analytical and technological developments over the past years have constituted MSI as a valuable asset in the bioanalysis toolbox.

Several MSI techniques exist for transferring the analytes from the tissue surface to the mass spectrometer. In this thesis, pneumatically assisted (PA) nanospray desorption electrospray ionization (nano-DESI) was used for ambient MSI of thin tissue sections. In PA nano-DESI MSI, molecules from the surface of the tissue section are desorbed into a liquid stream of solvent that is formed between two thin fused silica capillaries and electrosprayed directly into the mass spectrometer. The extraction solvent allows for addition of internal standards for matrix effects compensation and relative quantitation, and dopants for improved ionization efficiency of analytes as well as host-guest chemistry.

In this work, PA nano-DESI MSI was evaluated for its ability to provide insights into chemical mechanisms in health and disease. The effect of preconditioning agents on the membrane lipid breakdown after stroke as well as the effect of ischemia on acylcarnitine metabolism, which is involved in oxidation of fatty acids, was studied. These results provided valuable information into the chemical mechanisms that are induced during ischemia. Additionally, analytical insights are provided on the extraction abilities of various solvents used in PA nano-DESI. Further, analytical methodologies have been developed for analyzing challenging analytes, particularly light alkali metal ions (Na^+ and K^+), which cannot be directly detected by modern high resolution mass spectrometers, and prostaglandins, which exhibit many isomers that are not distinguishable through mass spectrometry alone. Finally, PA nano-DESI MSI was combined in one analytical platform with surface sampling capillary electrophoresis mass spectrometry (SS-CE-MS) to increase the coverage of information obtained from a single tissue section, *i.e.* elucidating isomeric species through electrophoretic separation.

Overall, this thesis adds unique insights into understanding ischemic stroke and presents novel analytical methodologies for analyzing prostaglandins, and Na^+ and K^+ ions. All developed methods are fully compatible with liquid extraction based MSI techniques which expands the range of applications.

Keywords: mass spectrometry imaging, ischemic stroke, mass spectrometry, isomers, spatial metabolomics, host-guest

Leonidas Mavroudakis, Department of Chemistry - BMC, Analytical Chemistry, Box 599, Uppsala University, SE-75124 Uppsala, Sweden.

ISSN 1651-6214
ISBN 978-91-513-1897-4
URN urn:nbn:se:uu:diva-511811 (http://urn.kb.se/resolve?urn=urn:nbn:se:uu:diva-511811)

Στον παππού Λεωνίδα

List of Papers

This thesis is based on the following papers, which are referred to in the text by their Roman numerals.

I. **Mavroudakis, L.**, Stevens, S.L., Duncan, K.D., Stenzel-Poore, M.P., Laskin, J., Lanekoff, I. (2021) CpG preconditioning reduces accumulation of lysophosphatidylcholine in ischemic brain tissue after middle cerebral artery occlusion. *Analytical and Bioanalytical Chemistry*, 413:2735–2745

II. **Mavroudakis, L.**, Duncan, K.D., Lanekoff, I. (2022) Host-guest chemistry for simultaneous imaging of endogenous alkali metals and metabolites with mass spectrometry. *Analytical Chemistry*, 94:2391–2398

III. **Mavroudakis, L.,** Lanekoff, I. (2023) Ischemic stroke causes disruptions in the carnitine shuttle system. *Metabolites*, 13:278

IV. **Mavroudakis, L.,** Lanekoff, I. (2023) Identification and imaging of prostaglandin isomers utilizing MS3 product ions and silver cationization. *Journal of the American Society for Mass Spectrometry*

V. ***Mavroudakis, L.,** *Golubova, A., Lanekoff, I. Spatial metabolomics platform combining mass spectrometry imaging and in-depth chemical characterization with capillary electrophoresis. *(Manuscript)*

*The authors contributed equally to the paper.

Contribution report

The author wishes to clarify his contribution to the research presented in papers I-V

I. Analyzed the data and wrote the manuscript with contributions from all co-authors.

II. Took part in planning of the study, performed the experiments, analyzed the data, and wrote the manuscript with contributions from all co-authors.

III. Responsible for planning the study, performed the experiments, analyzed the data, and wrote the manuscript with contributions from all co-authors.

IV. Responsible for planning the study, performed the experiments, analyzed the data, and wrote the manuscript with contributions from all co-authors.

V. Took part in planning of the study, performed the PA nano-DESI MSI experiments and part of CE-MS experiments, analyzed part of the data and contributed to the writing of the manuscript.

Papers not included in this thesis

Mavroudakis, L., Lanekoff, I. (2023). Matrix Effects Free Imaging of Thin Tissue Sections Using Pneumatically Assisted Nano-DESI MSI. In: Cole, L.M., Clench, M.R. (eds) Imaging Mass Spectrometry. Methods in Molecular Biology, vol 2688. Humana, New York, NY. https://doi.org/10.1007/978-1-0716-3319-9_10

Contents

Introduction 13

Mass spectrometry 15
- Basic principles 15
- Mass analyzers 16
  - Quadrupole 16
  - Linear ion trap 17
  - Orbitrap 18
- Tandem mass spectrometry 20
- Hybrid instruments 21

Sampling sources and ionization 23
- Secondary ion mass spectrometry (SIMS) 23
- Matrix-assisted laser desorption/ionization (MALDI) 24
- Electrospray ionization (ESI) 24
- Desorption electrospray ionization (DESI) 27
- Nanospray desorption electrospray ionization (nano-DESI) 27
- Pneumatically assisted (PA) nano-DESI 28
- Solvent versatility in nano-DESI and PA nano-DESI 29
  - Dopants and chemical derivatization 29

Mass spectrometry imaging 31
- Basic principles 31
- Data normalization 31
- Quantitation 32
- Spatial resolution 34
- Sample preparation 35

Surface sampling capillary electrophoresis 37
- Fundamentals of capillary electrophoresis 37
- Capillary electrophoresis mass spectrometry 38

Ischemic stroke 41

Scope 43

Discussion of findings 45
- Sampling solvent in PA nano-DESI 45

Selection of solvent system 45
Selection of internal standards for matrix effects compensation 48
Applications of (PA) nano-DESI MSI in ischemic stroke 51
Alterations of phospholipids in preconditioned ischemic mice 52
Alterations of acylcarnitines in ischemic mice 54
Development of analytical methods 56
Determination of Na^+ and K^+ using host-guest chemistry 56
Determination of prostaglandin isomers using tandem MS and silver cationization 58
Beyond the *m/z* in MSI: combination with SS-CE-MS for confident molecular annotations 60

Conclusions and future perspectives 63

Popular scientific summary 65

Populärvetenskaplig sammanfattning 67

Acknowledgements 69

References 71

Abbreviations

ADP	Adenosine diphosphate
ATP	Adenosine triphosphate
CAD	Collisionally activated dissociation
CE	Capillary electrophoresis
CID	Collision-induced dissociation
CMC	Carboxymethylcellulose
DC	Direct current
DESI	Desorption electrospray ionization
EOF	Electroosmotic flow
ESI	Electrospray ionization
FT	Fourier transform
FWHM	Full width at half maximum
GABA	Gamma-aminobutyric acid
HCD	Higher-energy collisional dissociation
ICP	Inductively coupled plasma
ICR	Ion cyclotron resonance
IM	Ion mobility
IR	Infrared
IS	Internal standard
ITO	Indium tin oxide
LA	Laser ablation
LC	Liquid chromatography
LIBS	Laser induced breakdown spectroscopy
LIT	Linear ion trap
LPC	Lysophosphatidylcholine
MALDI	Matrix-assisted laser desorption/ionization
MCAO	Middle cerebral artery occlusion
MS	Mass spectrometry
MSI	Mass spectrometry imaging
nano-DESI	Nanospray desorption electrospray ionization
NMDA	N-methyl-D-aspartate
OCT	Optimal cutting temperature
PA	Pneumatically assisted
PC	Phosphatidylcholine
PG	Prostaglandin

PLA_2	Phospholipase A2
PLC	Phospholipase C
RF	Radio frequency
SEM	Secondary electron multiplier
SIMS	Secondary ion mass spectrometry
SPE	Solid phase extraction
SS	Surface sampling
TEC	Tissue extinction coefficient
TIC	Total ion current
TOF	Time of flight
UV	Ultraviolet
XRF	X-ray fluorescence

Introduction

Bioanalytical chemistry is the scientific discipline that combines biology and analytical chemistry to explore the role of biomolecules in our everyday life. The term "biomolecules" is typically used for carbohydrates, proteins, lipids and nucleic acids but it can also include all molecules that are necessary for survival, *e.g.* metabolites. From immunoassays and electrochemistry to chromatography and mass spectrometry, bioanalytical chemistry is an essential discipline for understanding the chemical mechanisms of health and disease. Understanding biological mechanisms of action is of paramount importance for the development of treatments and improving the quality of life. For example, bioanalytical chemistry was involved in the development of self-tests for COVID-19 that anyone could undertake on their own as well as in the development of vaccines for the same disease.

Typical questions asked during bioanalysis are "*which biomolecule?*" and "*how much?*" Technological developments in the field of mass spectrometry, one of most sensitive analytical techniques, have shaped the answers that we can confidently provide to such questions. Analytical scientists are always striving to develop the most sensitive, the most specific and the fastest analytical technique possible. In many cases, a third question is asked; "*where is the biomolecule?"* Answering such question is important for understanding how drugs are metabolized in the body or how cancerous tissue affects its surroundings.

Mass spectrometry imaging (MSI) can provide spatially defined information on the abundance of detected biomolecules directly from tissue sections. Compared to traditional immunohistochemistry workflows, no labelling is required and thousands of molecules can be detected simultaneously. Over the past 30 years MSI has been maturing and it has proven to be an important technique for visualizing molecular distributions and deciphering biological mechanisms. Emerging technologies with enhanced sensitivity and specificity are always needed in MSI for pushing the boundaries of the field. In the work presented in this thesis, I have developed analytical methods for detecting challenging analytes such as Na^+ and K^+ which by means of modern high resolution mass spectrometers cannot be detected as well as prostaglandin isomers that due to their nature cannot be easily distinguished. Additionally, I have used MSI to further understand chemical mechanisms induced during ischemic stroke, one of the leading causes of death worldwide. Finally, the

combination of two mass spectrometry-based techniques was achieved for increased molecular coverage; MSI and surface sampling capillary electrophoresis mass spectrometry. This merging allowed annotation of analytes and the distinction of isomeric species with increased confidence. All methods developed in this thesis have been applied to actual biological samples to demonstrate their relevance and I anticipate more applications to emerge from such developments in the future.

Mass spectrometry

Basic principles

The basis of mass spectrometry (MS) is the manipulation of ions using electric or magnetic fields under vacuum conditions. Ions are measured based on their mass-to-charge ratio (*m/z*) and the detected signals are depicted in a mass spectrum where the intensity is plotted against the *m/z* of each ion. Mass spectrometers use a combination of direct current (DC) voltages and radio frequency (RF) voltages on various ion optics to move the ions from one part of the instrument to another or to trap them.[1] The amplitude and the frequency of RF voltage as well as the DC voltage are adjusted to maintain a stable ion trajectory. DC voltages are mainly applied to ion optics to direct ions towards a specific part of the instrument while RF voltages keep the ions suspended in the gas phase.[2–5]

The term mass accuracy in MS refers to how close the experimentally determined *m/z* is to the theoretical. Unless otherwise stated, in high resolution MS, the monoisotopic mass of a compound is mainly used. For example the compound with formula $C_{20}H_{32}O_5$ has a monoisotopic mass of 352.2249740 Da. Since it is ions that are detected in MS, the compound with formula $C_{20}H_{32}O_5$, that forms an adduct with Ag^+ ions, will have monoisotopic mass of 459.1295186 Da. Note that the resting mass of an electron (5.486×10^{-4} Da) is also accounted for in the monoisotopic mass of an ion.

An important parameter in mass spectrometric measurements is the mass resolution or mass resolving power (these two terms are used interchangeably). There are two ways of defining the mass resolution and both are acceptable as long as the method of calculation is specified.[6] The first definition uses $m/\Delta m$, where m is the mass of singly-charged ions depicted as a single peak in the mass spectrum and Δm is the full width at half maximum (FWHM) of the peak height. The second definition uses *m1/(m1-m2)*, where *m1* and *m2* are the masses of singly-charged ions present in the mass spectrum at equal height and at 10% overlap of the peak height. Instruments with high mass resolution can distinguish ions with small differences in their *m/z* which provides higher confidence in the identification of molecular formulas. For example, two molecules that differ by one double bond *e.g.* $C_{20}H_{30}O_5$ and $C_{20}H_{32}O_5$ and cationized with Ag^+ require high enough mass resolution to separate the peaks for $[C_{20}H_{30}O_5 + {}^{109}Ag]^+$ and $[C_{20}H_{32}O_5 + {}^{107}Ag]^+$ which are

separated by 0.01599 Da. For the separation of these two peaks (at 10% overlapping peak height) at least 28700 (*m1/(m1-m2)* at *m/z* 459.11353) mass resolution is needed.

Mass analyzers

Quadrupole

A quadrupole is a mass analyzer commonly used in mass spectrometers and consists of four parallel rods. Depending on the number of rods there can be hexapoles (6 rods), octapoles (8 rods) or decapoles (10 rods). The rods are arranged symmetrically around a center axis and those that are opposite of each other are electrically connected, thus, they experience the same voltage at each time point.[7,8] To maintain the ion beam trajectory, RF voltages that are phase shifted are applied on different pairs of rods so that when a pair of rods experiences maximum positive voltage, the other experiences maximum negative voltage (**Figure 1A**). A quadrupole that has only RF voltages acts as a transportation guide between different parts of the instrument.[5] If DC voltages are applied on top of RF, then the quadrupole can isolate specific ions. This occurs because a set of ions is stable within specific values of RF and DC voltages[5] (**Figure 1B**). By alternating those voltages, the isolated package of ions can be manipulated.

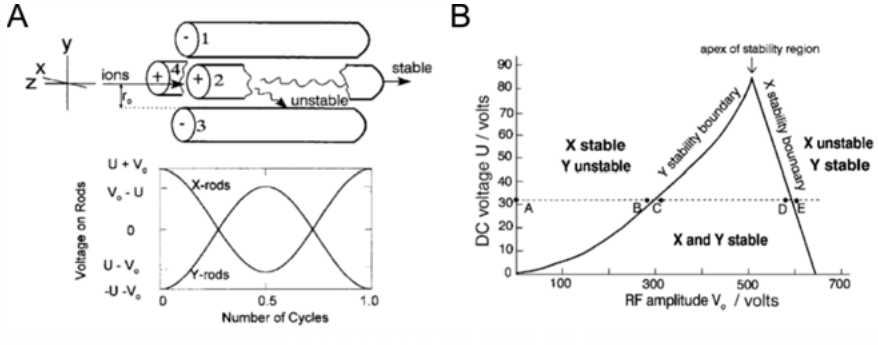

Figure 1. Schematic of the operation principle of quadrupoles in MS. A) Quadrupole mass analyzer and voltage applied on the rods. B) Stability diagram for a quadrupole where U denotes the DC voltage parameter and V_0 the RF voltage amplitude. A, B, C, D, and E represent ions that have different stabilities. Only C and D ions have stable trajectories. Reprinted from J. Chem. Educ. 1998, 75, 8, 1049 with permission from ACS.

Linear ion trap

The linear ion trap (LIT) is a 2D ion trapping device that is constructed by four rods forming a quadrupole (**Figure 2**). The RF and DC voltages applied on the rods can store, eject, isolate and fragment ions within the trap.[9] The main advantages of these devices are fast scanning speeds (hereby defined as Daltons per sec; Da/sec, where 1 Da = 1/12 of the mass of a carbon-12 atom), high storage capacity for ions and possibility for tandem MS (MS^n) experiments.[5] Fast scanning speeds are advantageous since many measurements can be collected over time and thus the signal-to-noise (*S/N*) ratio is improved. This improvement is achieved in cases of constant signal and random noise and the improvement is proportional to the square root of the number of measurements or measurement time.[10,11] Further, the high storage capacity of linear ion traps is beneficial for the stable trajectory of the stored ions. When too many ions are present in a confined area, space-charge effects occur which interfere with the stable trajectory of the ions, thus, reducing the quality of the measured data.[9] The space-charge effects can be observed in the broader shape of the *m/z* peaks and the deteriorated mass accuracy. Finally, MS^n experiments are valuable for structural elucidation. The basic principle is as follows: a set of ions can be isolated and stored in the LIT, fragmented due to resonance excitation and collisions with helium gas and subsequently another set of ions from the fragments can be selected for storage and further fragmentation.

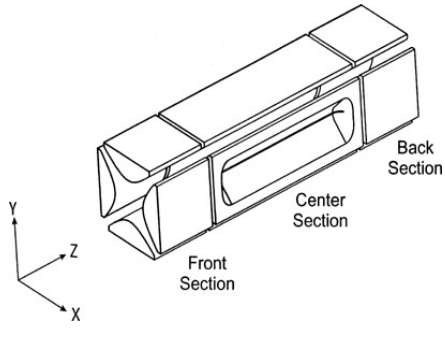

Figure 2. Schematic of a linear ion trap (LIT). Reprinted from J. Am. Soc. Mass Spectrom. 2002, 13, 6, 659–669 with permission from ACS.

Mass analyzers based on LIT designs operate at unit mass resolution *i.e.* they can separate ions with *m/z* difference of 1 unit.[9] Decreasing the scan rate can achieve better mass resolution. **Table 1** summarizes various scan modes of the LIT in the Orbitrap IQ-X instrument along with their corresponding scan rates

and peak widths. As it can be deducted, there is a trade-off between scan rate and peak width.

Table 1. Scan modes of the linear ion trap in the Orbitrap IQ-X mass spectrometer (From Orbitrap Tribrid Series, Hardware Manual, 80000-97537 Revision A, December 2022, Thermo Fisher Scientific)

Scan mode	Scan rate (Da/sec)	Peak width (FWHM)
Turbo	125000	≤ 3
Rapid	66666	≤ 0.6
Normal	33333	≤ 0.5
Enhanced	10000	≤ 0.35
Zoom	2222	≤ 0.3

Orbitrap

The orbitrap is a high-performance mass analyzer that traps ions in electrostatic fields. From its technological developments in the late 1990s to the commercialization in 2005, it has been instrumental to the development of mass spectrometers that offer high mass resolution without the high cost of purchase and maintenance associated with a Fourier transform ion cyclotron resonance (FT-ICR) mass spectrometer.

Orbitraps are composed of a spindle-shaped central electrode that is housed within two outer electrodes as shown in **Figure 3**. The construction of the device requires precision machining to maintain the control of the ion motion.[12] The inner and outer electrodes are electrically isolated from each other and serve two purposes: establishing the ion trapping field and image current detection. Thus, the orbitrap mass analyzer is both an analyzer and a detector. Externally generated ions are trapped in a curved linear trap called C-trap that operates as RF-only multipole. Subsequently, the ion package is ejected off-axis into the orbitrap where strong electric fields focus the ions and set them into a circular orbit around the central electrode. As the ions coherently oscillate around the central electrode, they form a thin rotating ring which induces a current on the outer electrodes that enables the image current detection. This signal is in the time-domain and to generate the mass spectrum Fourier transformation is applied.

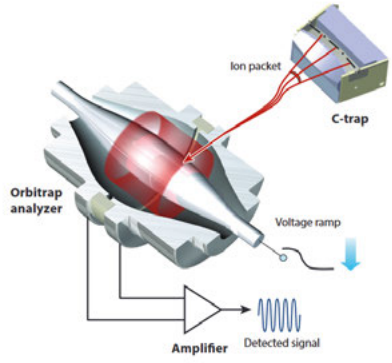

Figure 3. Cross section of the orbitrap mass analyzer and the C-trap device for injection of ions. Reprinted from Annual Review of Analytical Chemistry 2015 8:1, 61-80 with permission from Annual Reviews, Inc.

The orbitrap technology has refined the field of high resolution mass spectrometers by offering compact instruments at reasonable cost. However, it still has not exceeded the mass resolving power obtained by FT-ICR instruments. Recently, applications with mass resolving power ranging from 1.6 million to 7.9 million have been reported for FT-ICR MSI experiments.[13–15] However, such extremely high resolving power comes at the cost of long transient times, typically many seconds. The highest commercially available resolving power for orbitrap-based instruments is 1 million at *m/z* 200 (*e.g.* Orbitrap Tribrid IQ-X). Notice that all resolving powers mentioned above are for a specific *m/z*. This is due to the dependence of oscillation frequency and ultimately the resolving power on the *m/z* of the ion. This has an important implication; the resolving power is not constant throughout the *m/z* range. In orbitraps the resolving power is inversely proportional to the $(m/z)^{1/2}$ while in FT-ICR instruments it is inversely proportional to the *m/z*.[5] Thus, the loss of resolving power in higher *m/z* values is slower in orbitraps. Overall, constant developments in the orbitrap technology and instrument architecture push the boundaries of high resolution mass spectrometry.

Tandem mass spectrometry

The term tandem mass spectrometry, often abbreviated as MS/MS or MS^n, refers to the coupling of mass analysis stages that involve the fragmentation/dissociation of a molecular ion. Typically, a precursor ion is isolated by a mass analyzer and after activation or spontaneous dissociation, the product ions can be analyzed.[5] The detected product ions can provide information on the structure of the precursor ion, which is necessary for the identification of analytes.

MS/MS can be performed in time or in space. Tandem MS in space requires physically distinct mass analyzers for the fragmentation and analysis of product ions. Tandem MS in time requires an appropriate sequence of events that take place within the same mass analyzer. For example, a configuration of three quadrupoles in a row, termed as triple quadrupole or QqQ is a type of tandem MS in space. The Q denotes a quadrupole that acts as a mass analyzer while the q is an RF-only quadrupole. In the RF-only quadrupole, fragmentation takes place due to collisions with a gas *e.g.* nitrogen or argon. A typical MS/MS experiment utilizing a triple quadrupole instrument starts by isolating a defined *m/z* in the first Q followed by fragmentation in the second q and scanning of the product ions in the third Q. Tandem MS in time takes place typically in trapping devices such as linear ion traps which can store, eject, isolate and fragment ions.[5,9] Fragmentation takes place due to resonant excitation and collisions with helium gas present in the trap. This type of ion activation is termed collision-induced dissociation (CID) or collisional-activated dissociation (CAD). In a typical CID experiment, a precursor of interest is isolated and stored in the ion trap. An excitation frequency characteristic for the precursor *m/z* is applied which excites ions and results in fragmentation. The product ions are then scanned out from the ion trap by ramping the RF amplitude. Alternatively, a product ion can be isolated and further fragmented and the process can be repeated for *n* cycles (MS^n).

In this thesis, two ion activation modes were used for structural elucidation and studying fragmentation pathways; higher-energy collisional dissociation (HCD) and CID. HCD is a type of CID technique and is associated with instruments by Thermo Fisher Scientific that use an orbitrap mass analyzer. Precursor ions are transferred in the HCD cell (also termed as ion routine multipole) where they are accelerated due to voltage offset and collide with nitrogen gas. The product ions can be transferred back into the C-trap and eventually analyzed and detected by the orbitrap mass analyzer. The HCD cells are not capable of more than one cycle of fragmentation. This limits the fragmentation to MS^2 level in contrast with ion traps where up to MS^{10} can be achieved. However, hybrid instruments that contain an HCD cell and an ion trap are capable of MS^n experiments utilizing the HCD cell. In that case, the ion trap is used for storing and ejecting product ions while fragmentation takes place in the HCD cell.

The main differences between HCD and CID fragmentation lie in the extent of fragmentation and in the range of product ions that can be detected.[16] Typically HCD fragmentation results in more product ions compared to CID since energy is applied in all ions present in the HCD cell, thus, greater amount of information can be obtained from the MS/MS spectra. During CID, only the precursor ion is excited and fragmented. Further, the "one-third" rule in ion traps limits the detection of low *m/z* product ions[16], thus, potentially important product ions are not detected. In contrast, HCD cells do not have such limitation. This is demonstrated in **Figure 4** where the MS^2 spectra of the precursor *m/z* 468.18 (PGD_2-d_9 + $^{107}Ag^+$) were obtained with HCD and CID. The HCD spectrum contains more product ions and further low *m/z* ions such as 106.9046, corresponding to $^{107}Ag^+$ are detected while in the CID the low mass cut-off was *m/z* 124 (~1/3 of the precursor *m/z* 468.18). Older generations of hybrid orbitrap instruments allowed for HCD product ions to be detected only in the orbitrap, which is slower compared to detection in an ion trap, thus, increasing the duty cycle of the instrument. Newer generation of hybrid instruments allow for detection in the ion trap after HCD fragmentation up to MS^n level.

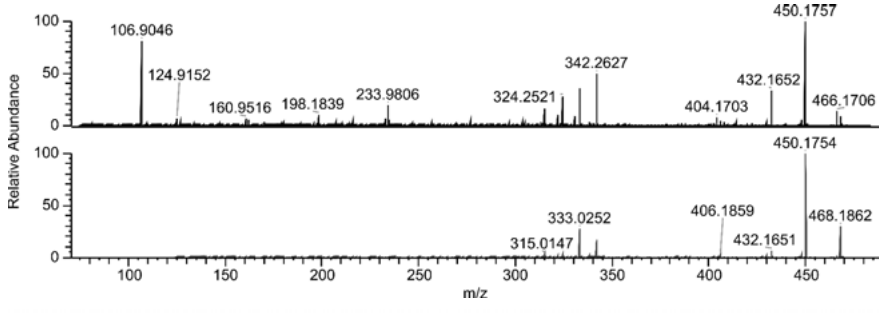

Figure 4. Comparison of HCD (top) and CID (bottom) MS^2 fragmentation of the product ion *m/z* 468.18 (PGD_2-d_9 + $^{107}Ag^+$).

Hybrid instruments

In the work done in this thesis, hybrid mass spectrometers from Thermo Fisher Scientific were used. These instruments combine two or more types of mass analyzers *e.g.* the orbitrap, linear ion trap or quadrupole. In **Paper I** an Orbitrap LTQ XL was used to acquire the data, in **Paper II, III & V** a QExactive was used while in **Paper IV** a Tribrid Orbitrap IQ-X was used. All these instruments have various multipoles and ion optics for transporting ions through the instrument. Note that to maintain the stable ion trajectory pumps are con-

stantly maintaining high vacuum (as low as 10^{-10} mbar inside the mass analyzer) throughout the instrument chambers. The Orbitrap LTQ XL is a hybrid instrument with a linear ion trap and an orbitrap as mass analyzers. The linear ion trap can store, isolate, fragment ions with the assistance of collision gas and send them either to the orbitrap for detection or to a secondary electron multiplier (SEM) detector. The QExactive has a quadrupole mass analyzer before the orbitrap and is capable of filtering the ions based on selected *m/z* values. Here, detection of ions takes place in the orbitrap. Finally, the tribrid IQ-X instrument combines all above technologies; it has a quadrupole for filtering selected *m/z* ions, a linear ion trap for storing, isolating and fragmenting ions which can be send either to the orbitrap for detection of to a dual-dynode detector. These architectures provide great flexibility to the experiments that can be conducted.

Sampling sources and ionization

Over the past 30 years of technological advancements in the field of MSI, several ionization sources have been used for elemental and/or molecular imaging.[17] For instance, laser ablation inductively coupled plasma (LA-ICP)[18] coupled with MS is a well-established technique for imaging of metals. However, elemental information can be also obtained without the use of mass spectrometers though laser induced breakdown spectroscopy (LIBS)[19] and X-ray fluorescence (XRF) spectroscopy.[20] Molecular techniques include matrix-assisted laser desorption/ionization (MALDI)[21], desorption electrospray ionization (DESI)[22] and nanospray desorption electrospray ionization (nano-DESI).[23] Several other laser-based techniques have been developed that have been recently reviewed.[24] Finally, secondary-ion mass spectrometry (SIMS) is a technique that can provide both elemental and molecular information.[25] Given the plethora of available techniques, combination of them provides larger coverage of both molecular and elemental information, a field known as multimodal imaging.[26,27] Given their extended use, the techniques of MALDI, DESI, nano-DESI and SIMS will be further introduced.

Secondary ion mass spectrometry (SIMS)

In SIMS, a high energy primary ion beam (*e.g.* Ar^+, Bi_3^+, Cs^+, O^-, C_{60}) is directed towards the sample and the interaction results in the ejection of secondary ions from the surface that are analyzed by the mass spectrometer. SIMS can provide both elemental and molecular information but due to the high energy deposition of the primary ion beam, mainly fragments of molecular ions are detected.[28,29] However, developments in the ion beams used have established SIMS as a valuable tool for detecting intact molecular species.[30] Additionally, it can be operated under dynamic mode where the energy of primary ion beam is altered resulting in deeper surface penetration.[31] Another variant of SIMS, nanoSIMS, provides the best achievable spatial resolution in MSI (50-100 nm).[32] Originally, SIMS was used with time of flight (TOF) mass spectrometers but further developments have incorporated high resolution mass analyzers.[33,34] Noteworthy, the 3D OrbiSIMS instrument[34]

combines the high spatial resolution of SIMS with high scan rates of TOF mass analyzers and high mass resolution of orbitrap mass analyzers.

Matrix-assisted laser desorption/ionization (MALDI)

MALDI-MSI was introduced in the 1990s[35,36] and is the most employed MSI technique today. For analysis, a sample on a conductive surface that has been previously sprayed with a MALDI matrix is irradiated with a laser beam (in the UV or IR region) and material is desorbed. The ionization process during MALDI has been proposed to proceed through the photochemical ionization model or the cluster ionization mechanism but it is still not well-understood.[37] During the photochemical ionization model, the MALDI matrix molecules absorb the energy from the laser and molecular ions of analytes are formed through charge transfer.[38] In the cluster ionization mechanism, protonated analyte polymers are already present in the MALDI matrix environment and are desorbed due to the laser irradiation[39]. Subsequently, gas-phase ions are produced by desolvation of neutral MALDI matrix molecules. Protonated (singly or multiply charged), deprotonated as well as adducts with metal ions can be produced during the MALDI process. Finally, the ions are transferred into the mass spectrometer for analysis. The choice of MALDI matrix is important as it has to possess certain properties for successful analysis.[40] Desorption and ionization of molecules is done under vacuum but atmospheric pressure MALDI has been also developed.[41] Noteworthy, is the development of MALDI-2 which uses a second laser to ionize the ablated material after irradiation with the first laser.[42,43] This has shown to improve the ionization efficiency of certain molecular classes and results in enhanced signals. Initially, TOF mass spectrometers were coupled to a MALDI source but over the past years of development several mass spectrometers have been used.[44]

Electrospray ionization (ESI)

A solution flowing through a capillary tube on which several kV (2-5) have been applied creates separation of charge at the surface of the liquid. The polarity of the applied voltage determines the polarity of ions which will be formed. For example applying positive voltage on the sample capillary produced positively charged ions. As the liquid exits the tip of the capillary a “Taylor-cone” is formed and once the electrostatic forces between the ions exceed the surface tension of the liquid (Rayleigh limit), droplets containing ions can detach from the liquid[45,46] (**Figure 5**). As the droplets are transferred towards the inlet of the MS the solvent evaporates, leading to the release

of ions from the droplets either through the ion evaporation or the charge residue model.[45,46] Briefly, the ion evaporation model, originally developed by Iribarne and Thompson[47,48], describes the release of ions from charged liquid droplets. As the droplets are being desolvated and shrinking (reaching a size of approximately 20 nm) and the charge density increases, solvated ions can be ejected from the droplet's surface.[46] In the charge residue model[49,50], highly charged droplets are constantly shrinking due to solvent evaporation until smaller charged droplets are formed due to electrostatic repulsions. Eventually, droplets that contain only one analyte ion are created. The general consensus is that the charge residue model favors molecular ions with weight larger than 1000 Da while smaller ions can be emitted from charged droplets through the ion evaporation model.[46] Recently, it was proposed that ions of disordered polymers such as unfolded proteins, can be formed through the chain ejection model.[51] In this model, the unfolded protein migrates towards the droplet exterior since the hydrophobic residues are now exposed and the interactions with the hydrophilic droplet interior are not favorable. Finally, the protein is ejected stepwise from the droplet in a mechanism similar to the ion evaporation model.

The introduction of ESI revolutionized the field of MS as it was realized that analytes can now be transferred from the solution phase to the gas phase for mass spectrometric analysis. The early works by Sir Geoffrey Taylor in 1964[52] and Dole *et al.*[50] laid the foundation for the development of ESI. In 2002, John B. Fenn (ESI) and Koichi Tanaka (MALDI) shared the Nobel Prize in Chemistry for their pioneering work in the development of soft ionization methods coupled with MS for the analysis of large biomolecules.[53,54]

ESI can operate with or without the assistance of nebulization gas.[55] At flow rates below 5 μL min^{-1}, little to no gas assistance is required to create a stable electrospray. When the flow rate is up to few tens of nL min^{-1} and no pumping of solution takes place, the technique is termed nanospray.[56,57] During nanospray (or nanoelectrospray), the initial smaller size of droplets that are generated (nanometers compared to micrometers in ESI) favors their desolvation compared to conventional ESI, thus, improving the signal quality. At higher flow rates effective desolvation of the droplets is assisted by a nebulizing or sheath gas. At even higher flow rates (> 0.1 mL min^{-1}), used mostly when coupling with liquid chromatography, a heated nebulizing gas can assist the desolvation. Effective solvent desolvation in ESI is not only beneficial for the production of gas-phase ions but also for the mass spectrometer as it can reduce the noise generated in the spectra. Incomplete desolvation typically favors the formation of gas-phase ions from analytes that reside mainly on the surface of the droplets, such as hydrophobic molecules *e.g.* amphiphilic analytes.[45,58] Since the droplet surface does not have infinite space for all analytes to reside, some analytes *e.g.* small metabolites such as amino acids reside in the inner part of the droplet where favorable hydrophilic interactions

take place. Thus, in the presence of analytes with various affinities for the surface of the droplets, discrimination effects in terms of ionization preference occur. These effects are collectively known as matrix effects.

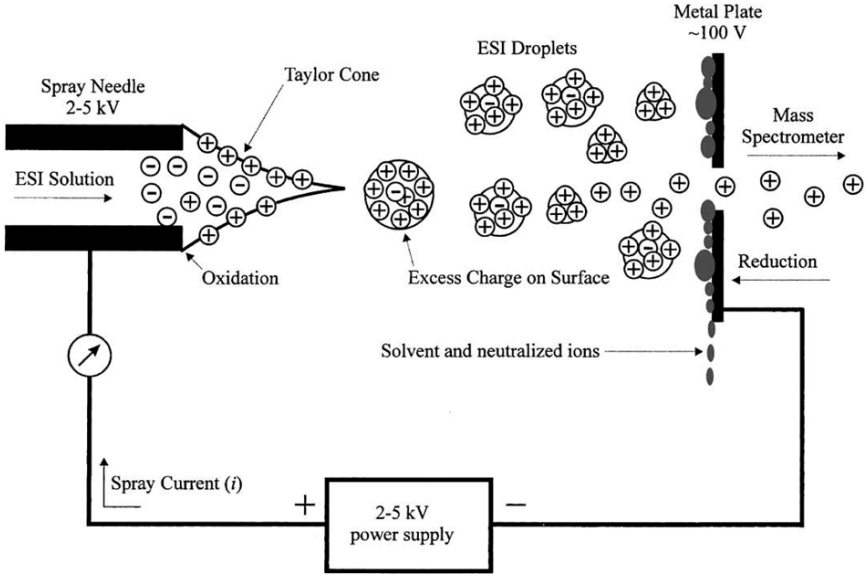

Figure 5. Schematic illustration of the ESI process. The solution of analytes is pumped through the spray needle which is held under high voltage. The charged droplets formed in the Taylor cone are evaporating as they move towards the inlet of the mass spectrometer. Reprinted from "Cech, N.B. and Enke, C.G. (2001), Practical implications of some recent studies in electrospray ionization fundamentals. Mass Spectrom. Rev., 20: 362-387" with permission from John Wiley and Sons.

Ionization with electrospray is considered a "soft" technique *i.e.* analytes do not undergo extensive fragmentation during ionization as opposed to "hard" ionization techniques such as electron ionization where fast moving electrons collide with the analytes. In ESI, adduct formation with H^+, Na^+, K^+, NH_4^+ or other alkali metal ions is the primary source of gas-phase ions in the positive mode while deprotonation (loss of H^+), adduct formation with Cl^- or $RCOO^-$ (R = H or CH_3) are the primary ions formed in the negative mode. Solvent additives or contaminants contribute to the formation of such adducts. Typically, most of the analytes are observed as singly charged ions but some analytes might carry two or several charges. For instance, proteins can accumulate several charges through adduct formation with H^+, NH_4^+ or alkali metal ions. The observation of multiply charged species with ESI was crucial for the development of methods that analyze proteins using mass analyzers that have limited high mass range.

Desorption electrospray ionization (DESI)

DESI was introduced in 2004, where it was demonstrated that a stream of charged droplets produced by ESI can desorb molecules directly from surfaces.[59] The impact of the charged solvent droplets causes the sputtering of molecular ions directly from the sample surface which are subsequently transferred into a mass spectrometer for analysis. The technique operates under ambient conditions which opened new avenues for analysis under atmospheric pressure. In contrast with MALDI, spraying of a laser-absorbing chemical matrix and conductive surface are not required. The solvent used for desorption is typically aqueous mixtures of organic solvents. The first application of DESI-MSI appeared in 2007[60] and since then many more applications have been described in biomedical research.[61–63] Since DESI is an ambient ionization technique, any mass spectrometer can be coupled.

Nanospray desorption electrospray ionization (nano-DESI)

Nano-DESI was reported for the first time in 2010 as a method of liquid-extraction surface sampling technique[64] and the first imaging application appeared two years later.[65] In nano-DESI, two thin fused silica capillaries (*e.g.* 50 μm I.D., 150 μm O.D.) are used for delivering a solvent onto the sample surface and subsequent electrospray. The solvent is propelled by a syringe pump through the first capillary. The second capillary is positioned at an angle relative to the first so that a liquid bridge is formed between them (**Figure 6**). The tip of the second capillary is positioned close to the inlet of a mass spectrometer where the vacuum inside the instrument assists with the transport of the liquid. High voltage (3-3.5 kV) is applied on the metal needle of the syringe delivering the solvent to facilitate electrospray at the second capillary that is close to the inlet of the mass spectrometer. When the liquid bridge comes into contact with the surface of the sample, molecules are dissolved in the solvent (usually mixture of water/methanol), ionized through ESI and transported in the mass spectrometer for analysis. Similar with DESI, there is no requirement for application of laser-absorbing matrix on top of the surface and use of conductive sample holders. The setup of a nano-DESI probe has been described thoroughly before[66] and the technique has been extensively used over the past years.[22,67,68]

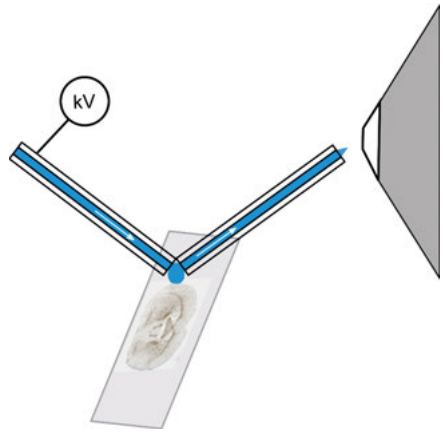

Figure 6. Schematic illustration of nano-DESI sampling from a surface where the white arrows indicate the flow of the solvent. The inlet of the mass spectrometer is shown on the far right. The individual elements are not in scale.

Pneumatically assisted (PA) nano-DESI

In 2017, Duncan *et al.* demonstrated that substituting the secondary capillary in nano-DESI with a nebulizer, improved the ionization of small metabolites and further showed less dependence on the probe-to-surface distance.[69] The improved ionization of small metabolites was attributed to better desolvation of the formed droplets due to the nebulization in combination with larger distance between the spray tip and the inlet of the mass spectrometer, which allows higher droplet desolvation. Further, the pulling action of the nebulizing gas due to the Venturi effect[70] creates a more stable flow through the secondary capillary which reduces the droplet instability due to distance variations. The technique was termed pneumatically assisted nano-DESI (PA nano-DESI) and since then its use for several applications has been evaluated.[71–73] We recently published a book chapter[74] where the construction and use of a PA nano-DESI probe is described in detail. Therefore, the probe will be described briefly in the next paragraph.

The PA nano-DESI probe uses a primary fused silica capillary connected to a syringe and syringe pump for solvent delivery. The choice of solvent depends on the experimental question and will be discussed further in the section "Selection of solvent system". Practically, the voltage difference between the

primary capillary and the instrument's inlet is applied directly on the metal needle of the syringe. The nebulizer that includes the secondary capillary is positioned at an angle of ~85° with respect to the primary capillary. The capillaries are aligned such that the primary is slightly below the secondary. The tip of the nebulizer is positioned in front of the inlet of the mass spectrometer at an angle of ~45°. These relative positions of the capillaries are similar to the nano-DESI described in the previous section. The solvent is pushed through the primary capillary and due to the flow of the nitrogen gas through the nebulizer, the liquid is aspirated towards the mass spectrometer. Then the gas flow is adjusted until a stable liquid bridge is obtained. The relative position of the primary and the secondary capillary is adjusted using micromanipulators to enable a stable liquid bridge. Further, the relative position and distance of the nebulizer compared to the mass spectrometer's inlet is optimized by using either the signal of standards spiked in the solvent or background ions. Overall, the process of optimization involves several parameters: the angle between the primary and secondary capillaries, the angle of the nebulizer's tip relative to the mass spectrometer's inlet, the position of the nebulizer's tip with respect to the inlet, the solvent flow rate, the electrospray voltage and the nebulizing gas flow rate. Once a stable and intense signal is established through electrospray in the mass spectrometer, the PA nano-DESI probe is maintained in that position throughout the experiment.

Although the PA nano-DESI probe does not operate in the high flow rate regime, the nebulizer is more effective at desolvating the formed droplets, as was discussed by Duncan *et al.*[69] It should be noted that despite the presence of "nanospray" in the name of PA nano-DESI and nano-DESI techniques, they not actually operating within the nanospray regime flow rates (a few nL min^{-1} to tens of nL min^{-1}).

Solvent versatility in nano-DESI and PA nano-DESI

Dopants and chemical derivatization

The versatility of the solvent in liquid extraction based MSI techniques such as nano-DESI and PA nano-DESI is reflected in the choice of the solvent and the addition of standards for matrix effects compensation and relative quantitation (discussed in detail in "Sampling solvent in PA nano-DESI"). Further, dopants can be added in the solvent for improved ionization and/or chemical derivatization. Weigand *et al.* added ammonium fluoride in the nano-DESI solvent and demonstrated improved signals for lipids in the negative ion mode[75] but the same dopant was not effective at improving the ionization of triglycerides in the positive ion mode.[76] Chemical derivatization of analytes with low ionization efficiency can improve their detection through the

formation of a product with a permanent charge or increased surface activity.[21,77–81] Further, incorporation of MS-friendly detergent in the nano-DESI solvent has enabled the native MS analysis of intact membrane proteins which previously were not accessible.[82–87]

Silver ions have been used for the increased sensitivity of olefins, prostaglandins and for isomeric differentiation of phospholipids and cannabinoids.[73,88–93] Primarily it has been hypothesized that silver ions interact with double bonds[89,94] and it was shown that no interaction occurs between saturated fatty acids and silver ions.[91] However, Lillja *et al*. demonstrated that saturated phospholipids can form adducts with silver ions[88] thus extending the capabilities of silver adduct formation. The isotopic signature of silver ions (^{107}Ag:^{109}Ag = 51.839:48.161) provides additional information for identification of molecules that form adducts with silver. A disadvantage of the isotopic signature of silver ions is that the signal for the formed adduct is split into two mass channels. To maximize the obtained signal, monoisotopic silver[73,88] has been used.

Mass spectrometry imaging

Basic principles

MSI is a powerful technique for visualization of molecular distributions directly from biological surfaces without labeling of the target molecules.[62,95–98] Understanding chemical mechanisms of disease is of utmost importance for the development of treatments. Due to the molecular heterogeneity of tissue, spatial information is valuable for deciphering mechanisms of action. For instance, elucidating the processes that lead to the distribution and availability of drugs within a tissue is essential for pharmaceutical research and developments.[62]

In MSI the essential experimental components include a sample on a surface, a sampling source, an ionization source and a mass spectrometer. The sampling and ionization can be taking place simultaneously (*e.g.* MALDI, SIMS, DESI) or they can be decoupled (*e.g.* nano-DESI, PA nano-DESI). Individual and known (*x,y*) locations of the tissue section surface are sampled/ionized in a pre-defined pattern until the entire surface has been sampled. Sampling can be done either in vacuum or under ambient conditions. During each sampling event, molecules from the tissue section are desorbed, ionized, and analyzed by the mass spectrometer. Each sampling location, termed as pixel, contains a mass spectrum that has a plethora of ions. The detected abundance of an ion of interest can be extracted from each mass spectrum and visualized in a 2D heatmap, referred to as ion image. This process is aided by the use of software where the user can select specific *m/z* ions for visualization.[99–101] Finally, MSI can also provide visualization in the 3D space when multiple 2D ion images are reconstructed.[102–104]

Data normalization

Normalization of data in MSI is important for eliminating variances during the analysis that are not related to biological changes. For example, during MALDI-MSI, inhomogeneous deposition of the laser-absorbing matrix causes signal fluctuation.[105] Additionally, due to the lack of a separation step in MSI, ionization suppression typically occurs during ionization. This is due to the different chemical environment of the tissue and is referred to as matrix effects. For efficient data normalization, internal standards with structures as

similar as possible to the analyte are the optimal choice.[105] Internal standards such as stable isotope labelled versions of the analyte are incorporated during the analysis to account for matrix effects (discussed in detail in section "Selection of internal standards for matrix effects compensation").

Normalization methods commonly used in MSI include normalization to the total ion current (TIC), internal standard (IS), matrix-related peak or endogenous species and tissue extinction coefficient (TEC). Normalization to the TIC is the most popular method in MSI due to its simplicity and ease of implementation. The method assumes that the ionization fluctuations caused by the tissue chemical environment will be reflected in the TIC and thus dividing the signal of an analyte with the TIC will compensate for this. Alternatives to the TIC are the median intensity of all peaks or using the median noise level.[106] Fonville *et al*. developed a variant of TIC normalization where biologically relevant peaks are utilized.[107] Lanekoff *et al*. demonstrated that TIC normalization does not account for matrix effects related to different salt composition of the samples.[108] Overall, careful consideration of the underlying matrix effects and the employed normalization routine is necessary for MSI experiments.

Normalization to the IS remains the most robust method for signal correction since the analyte and IS experience the same matrix effects during ionization. The internal standard can be applied directly on the tissue surface together with the laser-absorbing matrix (if any).[105] Alternatively, for liquid-based extraction techniques such as nano-DESI, the IS can be directly added in the solvent. This approach enables pixel-wise normalization *i.e.* the internal standard is present in the same spectrum as the target analyte. Signal normalization can be achieved by the use of peaks originating from the sprayed laser-absorbing matrix (for MALDI-MSI) or carefully chosen endogenous species that are highly abundant and homogeneous over the tissue.[105] Finally, the calculation of tissue extinction coefficients has been demonstrated for normalization.[109,110] In this method, a standard is sprayed homogeneously over the tissue section and the relative ionization suppression is calculated for various morphological regions compared to an area where there is no suppression (*i.e.* empty glass slide). Overall, robust data normalization is a necessary step for reporting unbiased results as well as transitioning to quantitative investigations.

Quantitation

Quantitation in MSI is important for deeper understanding of biological systems. However, it requires careful consideration of several factors, such as matrix effects due to tissue heterogeneity, normalization of data and extraction efficiency of the analytes from the tissue. The latter is necessary for absolute quantitation. Most often, relative quantitation strategies are applicable in MSI

where different tissue regions are directly compared after appropriate data normalization. The biggest challenge in quantitative MSI is mimicking the biological environment of the sample in order to create the same ionization conditions for the standards. An interesting approach that mimics the native tissue environment is the creation of mimetic tissue models or tissue surrogates with spiked standards.[111,112] Tissue is homogenized together with standards, frozen, sectioned and analyzed. Finally, the investigated tissue can be analyzed and the signals obtained from the mimetic tissue and the native tissue can be compared. Essentially, this approach is similar to a matrix-matched calibration in traditional liquid chromatography (LC) experiments where the standards are present in the same matrix as the actual sample to experience the same matrix effects during analysis.[113]

Several strategies have been developed for obtaining quantitative results from MSI experiments. For example, standards can be spotted adjacent to the tissue section, directly on top of or under a tissue section, or premixed with a complex matrix and then spotted on the tissue.[114,115] Thus, the standards and the endogenous analytes are desorbed and ionized at the same time. The spotting on top of the tissue method is reported to outperform the rest[116] but this approach requires a large enough morphological region on the tissue section for spotting of various standards. Further it is not clear whether the standard is mixed adequately with the sample matrix during the spotting. This approach, however, does not account for the extraction efficiency of the endogenous analyte. Regardless, quantitation in MSI can be significantly improved when isotopically labelled standards are used.[117] Another challenge for quantitation in MSI is the validation of the results. Typically, the results from MSI are compared with analysis using a gold-standard technique such as liquid chromatography mass spectrometry (LC-MS). However, it is not possible to analyze exactly the same tissue area with LC-MS and with MSI and thus most approaches use whole tissue sections. Nonetheless, studies have shown good agreement between quantitative MSI and LC-MS results.[105,117]

In nano-DESI and (PA) nano-DESI MSI, standards can be directly added in the solvent and ionize simultaneously with the target analytes, thus, experiencing the same matrix effects. When appropriate standards are used (ideally stable isotope labelled versions of the analytes) the signal normalization and quantitation is feasible.[118] Quantitation is achieved by using the one-point calibration technique[119,120] where the concentration of the standard spiked in the solvent generates intensity similar to the analyte. The concentration of the endogenous analyte is determined using the following equation:

$$C_{end} = a \times \frac{I_{end}}{I_{std}} \times C_{std} \quad (1)$$

where a is the response factor between the endogenous analyte and the standard (*i.e.* a measurement of how similar the ionize), I_{end} and I_{std} are the signal intensities for the endogenous analyte and standard, respectively, and C_{std} is the concentration of the standard spiked in the solvent. When stable isotope labelled versions of the analyte are used, the response factor is assumed to be 1. This method enables pixel-wise quantitation but the extraction efficiency of the endogenous analytes is not accounted for and thus absolute quantitation is not possible. It has been recently shown that multiple labelled compounds can be used simultaneously to create a calibration curve and quantify pixel-by-pixel.[121] In conclusion, accurate quantitation in MSI is challenging and requires detailed understanding of the underlying factors affecting the analyte signal.

Spatial resolution

In MSI the spatial resolution is typically defined by the size of the sampling area. For example, in laser-based techniques, the diameter of the laser spot and the movement of the sample stage dictate the spatial resolution.[24,122] In liquid-based extraction techniques, the size of the sampling droplet or plume (in case of DESI) is of importance. For techniques where continuous extraction/desorption of molecules is done (*e.g.* nano-DESI and DESI), the scan rate of the mass spectrometer, the movement speed of the sample holder and the stepping size between adjacent lines are needed to estimate the pixel size. However, the spatial resolution, which is different than the pixel size, is determined by the diameter of the liquid bridge between the two capillaries in the case of nano-DESI[123] and the scan rate of the mass spectrometer. The size of the liquid bridge is determined by the diameter of the fused silica capillaries, the solvent flow rate, and their relative position.

Advancements in laser technology drive the laser-based techniques towards higher spatial resolution and now they can routinely achieve < 10 μm.[96] In liquid-based extraction techniques, smaller droplet size or plumes are required, which can be experimentally challenging to achieve, with the best reported being ~10 μm.[124] To estimate the spatial resolution, both software/data and experimental methods have been developed.[99,122,125] In nano-DESI MSI, the pixel size is typically reported as the scan rate of the mass spectrometer divided by the sample motion speed for the x-axis and the stepping size for the y-axis. For example, in an analysis where the sample is moved under the nano-DESI probe at 40 μm s^{-1}, the mass spectrometer acquires data at 2 Hz and the stepping size is 150 μm, the final pixel size is 20 μm x 150 μm. Estimation of the spatial resolution is typically done by determining the distance that the signal has increased from 20% to 80% relative intensity in areas where there are chemical gradients or distinct morphological features.[99,123,126,127]

Impressive spatial resolution in MSI creates highly detailed ion images and can reveal important morphological features.[96] However, this come at the cost of analysis time and most importantly decreased sensitivity of the MS detection. Unsurprisingly, sampling less material yields less ions that enter the mass spectrometer, thus, low abundance features can go undetected. This is additionally exaggerated by the fact that the ionization efficiency rate is not 100%. Further, confident identification of the analytes is not possible without tandem mass spectrometry, which requires adequate signal intensity to provide good quality data. Bulk analysis of tissue extracts for confirmation of annotations is possible but it can be argued that the correlation between spatial position and analyte identity is lost. Constant improvements in the ionization efficiency of molecules (*e.g.* MALDI-2[42]) aim to alleviate this problem. Both computational and hardware methods have also demonstrated increased throughput of analysis with minimal loss of spatial resolution.[128]

Sample preparation

In MSI experiments, thin tissue sections can be analyzed to obtain the spatial distribution of analytes. These thin tissue sections are obtained from organs that have been previously snap-frozen to prevent molecular degradation. Snap-freeze is an important step and takes place immediately after the organ removal to halt enzymatic activity and is usually done with liquid nitrogen or dry-ice chilled isopentane. The latter is preferred over liquid nitrogen due to its better cooling rate[129] and also liquid nitrogen boils which created an unpredictable freezing pattern, which can distort the tissue morphology.[130]

Typical thickness of tissue sections lies between 10-20 µm but sections at 3-5 µm have been analyzed.[129] Tissue sections as thin as 2 µm showed better quality data compared to thicker ones and this was attributed to better charge dissipation during the MALDI process and more efficient lipid removal during washing.[131] However, the increased fragility of such thin tissue sections needs to be considered. Thus, typical tissue thickness used throughout the experiments in this thesis was 10-12 µm. The sectioning of tissue in this work was done using a cryotome that controls the temperature of the chamber and the blade. These temperatures are tissue dependent and require optimization prior to sectioning. For example, for brain sectioning temperatures of -20 °C in the chamber and the blade were found to deliver good quality tissue sections. Then the tissue is mounted on the holder of the cryotome using a small amount of water. In traditional histological experiments, the tissue is embedded in optimal cutting temperature (OCT) medium.[129] However, the contamination of the tissue section by OCT is detrimental to the quality of data obtained as severe signal suppression by the contaminants occurs in the mass spectra.[132,133] If the organ requires embedding in a medium, water, gelatine or carboxymethylcellulose (CMC) can be used.[129]

Thaw-mounting of the tissue section is the most common method for transferring the tissue section onto the surface. The choice of surface depends on the MSI technique used as some require the surface to be conductive. One example of conductive surface are indium-tin oxide (ITO) coated glass slides that are used in MALDI MSI. For nano-DESI imaging there is no requirement for surface conductivity, thus, regular glass microscope slides are typically used. After the tissue section has been thaw-mounted on the glass slide, it can be stored in -80 °C until analysis. It should be mentioned that long-term storage of tissue sections on glass slides should be avoided.[129] It has been reported that long-term storage up to one year showed no significant molecular degradation but more than that peptides and proteins were affected. For analysis, the tissue section is typically subjected to vacuum desiccation or rapid thawing to avoid condensation. Overall, sectioning, storage and handling of tissue sections is detrimental to the quality of the data obtained.

Surface sampling capillary electrophoresis

Fundamentals of capillary electrophoresis

Capillary electrophoresis (CE) is a separation technique where charged analytes are separated based on their movement in an electric field through a thin fused silica capillary. In CE the electrophoretic mobility of the analytes is the basis for their separation.[134] This property is characteristic of each ion in a medium and is determined by the charge and size of the ion. The electrophoretic mobility is proportional to the ion's charge and inversely proportional to the viscosity of the medium and the ion's radius. Thus, highly charged small ions have higher mobility than large, minimally charged ions. Compared to traditional separation methods such as liquid or gas chromatography, in CE there is no need for a stationary phase with which the analytes interact.

In a typical CE experiment, a sample in liquid form is loaded in the separation capillary usually by applying pressure (hydrodynamic injection) or by applying voltage (electrokinetic injection). The ends of the capillary are dipped into an inlet and outlet reservoirs containing an appropriate background electrolyte (**Figure 7**). The inlet and outlet reservoirs are connected to a high voltage power supply that provides the electric field for the separation of analytes in the capillary. A detector is usually placed towards the end of the separation capillary for detecting the signal from the separated analytes.

A fundamental aspect of CE for the movement of charged species through the capillary is the electroosmotic flow (EOF). Typically, silica capillaries under aqueous conditions possess exposed silanol groups (SiOH) that can be in the anionic form (SiO^-). Counterions in the electrolyte solution, typically cations, accumulate near the negatively charged capillary wall and form a thin wall. When the electric field is applied across the capillary, the movement of the solvated cations from the positive inlet towards the negative outlet (**Figure 7**) causes the bulk liquid to move as well. The movement of the EOF causes the migration of all species within the capillary towards the same direction. Cations migrate the fastest towards the negatively charged outlet (cathode) and they are arriving to the outlet faster than the bulk EOF. Anions are attracted by the positively charged inlet (anode) but due to the movement of the EOF towards the cathode they are still following the same direction. However, they are considerably slower than the bulk EOF. Finally, neutral species follow the same direction as the EOF but they are not separated from each other.

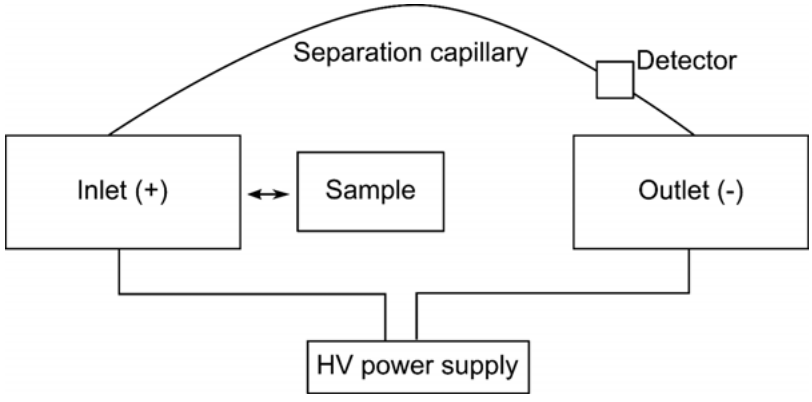

Figure 7. Schematic illustration of basic CE components. HV: high voltage

Capillary electrophoresis mass spectrometry

Among the most common detection methods in CE are those based in spectroscopy and electrochemistry.[135] These detection methods are sensitive and offer the possibility for on-line detection. Mass spectrometry can be coupled to CE for increased confidence in the identification of analytes.[136] Very low sample volumes (nanoliters) can be analyzed with CE and in combination with the increased identification confidence through MS, CE-MS is a valuable tool for the analysis of biological samples. However, coupling CE to MS requires the presence of a sheath liquid which leads to dilution of the analyte bands and reduces the sensitivity. The sheath liquid is necessary for minimizing the formation of hydrogen and oxygen gas bubbles due to electrolysis which negatively affects the analysis.[137] Sheathless interfaces for CE-MS are an active field of research to circumvent the analyte dilution.[138]

Analysis of biological samples using CE-MS requires the sample to be in a liquid form. Therefore, intact tissue sections that contain valuable spatial information of analyte localization are not directly compatible. Using laser capture microdissection followed by LC-MS analysis has been reported before for regional analysis.[139] Further, direct surface sampling using solvent and LC-MS analysis provides spatially defined information from tissues.[140,141] However, spatially defined analysis using CE offers the advantage of higher separation efficiency compared to LC.[136] For that, Duncan *et al.* developed the surface sampling (SS) CE-MS which enabled the sampling directly from thin tissue sections.[142] Further developments and optimization of SS-CE-MS by Golubova *et al*. demonstrated that SS-CE-MS is a versatile tool that can be used for the analysis of lipids, proteins and polar metabolites.[143]

A major advantage of CE-MS is the capability for separating isomers and isobars even with enantioselectivity.[143–146] In direct infusion MS-based approaches such as MSI, pre-separation of analytes is omitted and thus isomers and isobars are not resolved by *m/z* alone.

Ischemic stroke

Ischemic stroke is one of the primary causes of death and disability worldwide. It accounts for 87% of the stroke incidents and atherosclerosis is the main cause of it.[147] According to the American Heart Association, one person suffers from a stroke every 40 seconds.[147] The fatty deposits obstruct the blood supply to the brain causing a lack of nutrients and oxygen.[148] This has adverse effects for the brain cells and ultimately leads to inflammation, oxidative stress, ionic imbalance and apoptosis. During ischemia the lack of oxygen needed for oxidative phosphorylation leads to the rapid consumption of adenosine triphosphate (ATP) and release of glutamate by the neurons.[149] The release of glutamate has detrimental effects for the neurons causing the activation of N-methyl-D-aspartate (NMDA) receptors.[150,151] These receptors allow calcium ions (Ca^{2+}) to enter the cells exaggerating the ionic imbalance. Further, membrane depolarization occurs and the normal function of Na/K ATPase is severely disrupted.

Potassium and sodium ions levels are, under physiological conditions, tightly regulated through the Na/K ATPase.[152] Specifically, inside the cells, the levels of potassium are higher than sodium under normal conditions.[153] During ischemia, potassium exits the cells while sodium enters at the same time causing ionic imbalance.[154,155] Additionally, Ca^{2+}, which are typically maintained at low levels intracellularly, are entering the cells causing activation of calcium-dependent proteases, lipases and DNases.[151,156] For example, calcium-dependent phospholipase A_2 (PLA_2) and phospholipase C (PLC) are activated and degrade membrane phospholipids. Ultimately, activation of such enzymes results in cellular apoptosis. The ionic imbalance due to high intracellular levels of Ca^{2+}, Na^{+} and adenosine diphosphate (ADP) has deleterious effects for the mitochondria through the production of reactive oxygen species, thus, affecting the energy production.[157]

Treatment of acute ischemic stroke requires effective recanalization and reperfusion to salvage the brain tissue. The timeline is very important and the most established treatments are intravenous thrombolysis using recombinant tissue plasminogen activator (effective window of 4.5 hours) and endovascular thrombectomy (effective window of 6 hours).[158] Both methods aim to dissolve the formed clot so blood flow can be restored. An alternative treatment that “remains one of the holy grails of acute ischemic stroke ther-

apy"[159] is neuroprotection. This therapy aims at minimizing neuronal damage that occurs during reperfusion and could be achieved with or without the administration of pharmacological agents. However, the abovementioned treatment therapies are administered after the occurrence of stroke and require early recognition of the symptoms. On the other hand, ischemic preconditioning aims at "preparing" the brain for a subsequent ischemic stroke by triggering defense mechanisms that typically occur during an actual ischemic stroke.[160] In all cases, deep understanding of the underlying chemical mechanisms in ischemic stroke is of vital importance for the development of treatments.

To study ischemic stroke, the most common experimental model is the middle cerebral artery occlusion (MCAO).[161] This model causes disruption of the blood flow to the brain by inclusion of a monofilament into the artery and it can be used for permanent or transient ischemia. In this model, one hemisphere of the brain is damaged while the other remains largely unaffected, thus providing a damaged and a control region within the same tissue section.[162] After the filament is removed, the blood flow is restored (reperfusion) and the time range of reperfusion is typically between 1 hour and 2 hours. Restoration of the blood flow is necessary for salvaging ischemic tissue, however, it results in ischemia/reperfusion injury where, paradoxically, the damage is further exaggerated.[163] This experimental stroke model resembles the human stroke in terms of localization but it has been heavily criticized for its translational aspects. The reason for the criticism lies in an inherent problem with this model; in human stroke vessel occlusion is rarely complete. Nonetheless, MCAO has provided substantial amount of knowledge regarding the pathophysiology of ischemic stroke and has been valuable source of material for research and method development in this thesis.

Scope

The aim of this thesis was to add to the portfolio of analytical methods in MSI and thus increase its versatility and range of applications. Further, it was important to demonstrate that MSI is not an isolated field but rather a great tool in understanding chemical mechanisms in health and disease. The work presented here is divided into two parts: applications and method developments. First, applications of MSI in the analysis of biological samples were important for gaining insights into mechanisms of action in ischemic stroke. This work utilized the power of MSI to provide spatially defined information and highlighted its relevance in the field of bioanalysis. Second, development of analytical methods that are compatible with MSI of challenging analytes are presented. Each method has been extensively evaluated and most importantly applied in a biological sample to showcase its importance and relevance. Finally, some unpublished results are presented and discussed in the context of solvent selection in PA nano-DESI MSI. The solvent tunability of this MSI technique is one of the biggest advantages and in-depth knowledge of the underlying mechanisms of extraction/desorption/ionization are of utmost importance for reaching the full potential of the analysis.

Discussion of findings

Sampling solvent in PA nano-DESI

Selection of solvent system

The choice of solvent for sampling using PA nano-DESI typically follows the basic rules of extraction in chemistry. The molecular classes to be investigated influence the choice of solvent. However, there are two more factors to consider when selecting a solvent. First, the selected solvent should be compatible with ESI-MS so that a stable spray can be obtained.[164] Second, the surface tension and affinity of a solvent for a surface influences the stability of the formed liquid bridge. Solvents with low surface tension tend to form unstable liquid bridges when in contact with a hydrophilic glass surface *e.g.* acetone. Non-polar organic solvents such as chloroform, hexane, toluene or dichloromethane are typically avoided as they are not considered "ESI-friendly".[164] However, it has been shown that when mixed with polar organic solvents such as methanol and acetonitrile, the detection of non-polar triglyceride species with nano-DESI is improved.[76]

The most commonly used solvent system in nano-DESI applications is methanol:water 9:1 (v/v)[66] and this was the solvent used in **Paper I, III & V**. This solvent system is able to extract both metabolites and lipids at the same time. The use of solely water as solvent has been described using the PA nano-DESI probe which enabled the imaging of highly polar analytes.[69] Pure methanol was used as the PA nano-DESI solvent in **Paper II** since the affinities for Na^+ and K^+ for methanol:water mixtures were not available in the literature. When analyzing tissue sections that contain large amounts of NaCl and/or KCl due to the normal cell environment, the extraction of these salts can cause problems. One such case is when silver ions are added in the nano-DESI solvent to improve the ionization of specific molecular classes.[73,88,91,165,166] The presence of Cl^- leads to the formation of AgCl(s) which consumes the available Ag^+ and thus diminishes the adduct formation with analytes. Further, AgCl(s) builds up on the spray capillary tip and eventually leads to clogging. Thus, acetonitrile is typically preferred over methanol and water due to lower solubility of NaCl and KCl.[91] In **Paper IV** acetonitrile:methanol 9:1 (v/v) was used as the solvent system to minimize extraction of NaCl and KCl. As it can be concluded, the choice of solvent in nano-DESI is a multivariable problem where a systematic investigation of the different

solvent systems and their extraction capabilities is lacking. Recently, Lin *et al.* investigated the extraction efficiencies of various solvents for lipid analysis (fatty acids, phospholipids, ceramides and cardiolipins) and concluded that optimization of the solvent system in terms of intermolecular interactions and extraction time affected the obtained lipid profiles.[167]

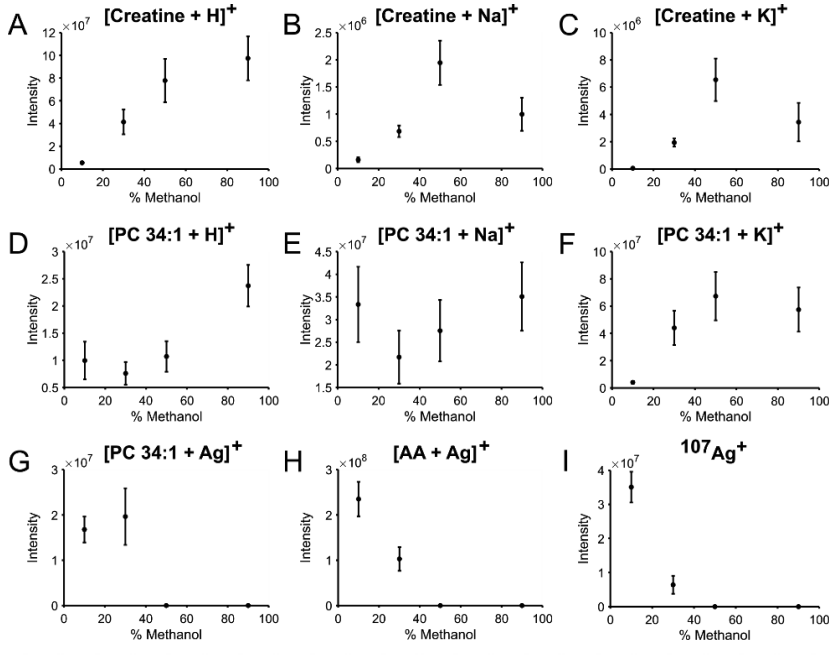

Figure 8. Average intensities (n = 20) of various ions from line scan over a mouse brain tissue section using PA nano-DESI MS with different mixtures of methanol/acetonitrile. All solvents contained 10 ppm $^{107}Ag^{+}$. Error bars represent the standard deviation of the average intensity. AA: arachidonic acid, PC: phosphatidylcholine

In an effort to systematically evaluate the different solvents and their extraction capabilities with PA nano-DESI MSI, different mixtures of methanol/acetonitrile were tested. These solvents were selected as they are commonly used with ESI-MS. The data were obtained in consecutive lines over a mouse brain tissue section and 20 scans were averaged, representing similar chemical environment. Small polar organic molecules such as creatine, which is abundant in brain tissue, was detected with higher intensity when the methanol portion was increased (**Figure 8A-C**). This observation is attributed to a higher extraction efficiency of methanol and/or more efficient desolvation during ESI. Increasing the methanol content does indeed result in higher signals for the protonated adduct of creatine, as shown in **Figure 9**. Overall, higher extraction

efficiency of methanol compared to acetonitrile and better desolvation during ESI contributed to the increased signals for polar analytes such as creatine.

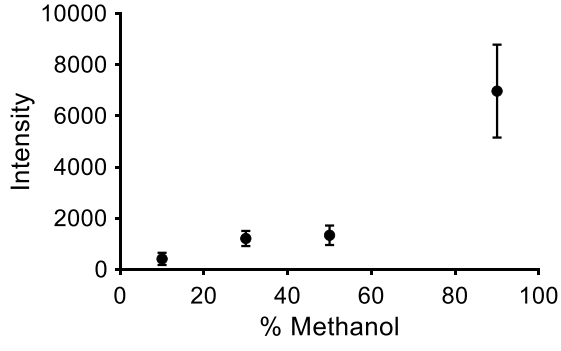

Figure 9. Effect of methanol proportion in ESI-MS. Shown is the signal for [Creatine + H]$^+$ obtained from solutions that have various proportions of methanol/acetonitrile, 10 ppm $^{107}Ag^+$, 0.2% formic acid and 500-times diluted rat brain extract. All samples were analyzed under identical ESI-MS conditions.

In the case of alkali metal ion adducts (Na^+ and K^+), the results were not as straightforward. The protonated adduct of PC 34:1 (**Figure 8D**) was detected with the highest intensity when 90% methanol was used indicating a combination of increased extraction efficiency of the solvent, increased proton donor abilities due to the presence of the protic solvent methanol, and increased desolvation of the solvent. The sodiated adduct of PC 34:1 (**Figure 8E**) did not show a clear trend which could be explained by the constant presence of Na^+ impurities in the solvents. The potasiated adduct (**Figure 8F**) provides evidence for increased extraction of K^+ with increased content of methanol. Similar trends were observed in the case of creatine (**Figure 8B-C**). The balance between protonated, sodiated and potasiated adducts is dependent on the chemical environment and solvent impurities and it is not always easy to control.[168,169] Increased signals for phospholipids such as PC 34:1 with higher methanol content should induce more matrix effects, which could explain the fact that the signal for [Creatine + H]$^+$ is almost reaching a plateau in **Figure 8A**. The latter could also be attributed to saturation of the extraction solvent with creatine. Nonetheless, the desolvation and the extraction effect are overpowering the ion suppression due to matrix effects from phospholipids.

The data shown in **Figure 8** demonstrate that there is a trade-off between higher detected intensity for small molecules (*e.g.* creatine) and availability of silver ions. It became clear that when the percentage of methanol was more than 30% (70% acetonitrile) the extraction of NaCl and KCl was diminishing

the amount of silver ions either detected as free or as adducts with biomolecules (**Figure 8G-I**). It was hypothesized that with 20% methanol – 80% acetonitrile we would still retain enough silver ions to form adducts with molecules while at the same time extracting small molecules. However, the PA nano-DESI MSI experiment of a mouse brain tissue section with that solvent was unsuccessful. After 3 hours of data acquisition the capillaries were clogged by AgCl(s) and the electrospray was highly unstable. Further, since the 30% methanol – 70% acetonitrile solvent was able to extract small molecules and still retain free silver ions or form adducts of molecule with silver (**Figure 8**), the substitution of methanol by other alcohols was considered. The hypothesis involved lowering the extracted amount of NaCl and KCl due to less polar alcohol but still extracting organic molecules.[170] However, both ethanol and isopropanol were not able to extract small metabolites such as amino acids while signals for highly abundant species such as creatine were 4-fold lower compared to methanol. Additionally, the stability of the liquid bridge was negatively affected by substituting methanol with ethanol or isopropanol. Thus, the presence of methanol was deemed necessary. The solvent with 90% acetonitrile – 10% methanol was still considered the best option when using silver ions.

Selection of internal standards for matrix effects compensation

The ionization of molecules during ESI is dependent of the chemical environment. Due to the nature of the ESI process, molecules with high affinity for the surface of the droplets will outcompete molecules with lower affinity which leads to matrix effects. While the latter usually results in ionization suppression, enhancement of ionization has also been observed.[171,172] Since the droplets during ESI can undergo uneven fission, mass and charge separation becomes important, leaving molecules in the interior of the droplets uncharged.[58,173,174] This is a well-known phenomenon in ESI-MS and if not accounted for, biased results are reported.[45] One way to alleviate the matrix effects is by improving the desolvation process of electrospray. This was originally demonstrated with nanospray where the initially smaller droplets can produce ions in the gas phase directly without relying on the fission of the droplet.[175] If matrix effects cannot be avoided, then identification and compensation is important. This can be achieved by including internal standards during the analysis that ionize simultaneously with the analyte ions and thus experience the same matrix effects. Internal standards have been used extensively in ESI-MS for quantitative investigations.[176,177] Direct-infusion approaches require the use of internal standards for correction of matrix effects. However, when a chromatographic separation or sample clean-up (*e.g.* solid phase extraction, SPE) is employed, then the matrix is separated by the

analytes. Since MSI experiments operate without any chromatographic separation or sample clean up prior to analysis, it is important to identify and compensate for the ionization suppression or enhancement of analytes.

Identification of matrix effects is typically carried out by comparing the response of an analyte with and without the matrix being present. In MSI approaches, identification of matrix effects is aided by the use of standards that are either spiked in the solvent for liquid-based extraction MSI techniques or sprayed over the tissue section for desorption-based techniques.[178] The analysis of complex tissue samples usually results in two types of matrix effects: salt-related and chemical composition-related.[178] Salt-related matrix effects are caused by the natural presence of NaCl and KCl in the cells of the tissue and the preference of molecules to form adducts with Na^+ and K^+. Chemical composition-related matrix effects are due to the chemical environment of the tissue. This typically results in ionization suppression of analytes because of the presence of molecules from the tissue that have high surface activity *e.g.* phospholipids. It has been demonstrated that failing to account for the matrix effects caused by the abundance of Na^+ and K^+ in the tissue results in mixed conclusions regarding the abundance of molecules (**Paper I**).[108] Further, Bergman *et al*. showed that the ionization of small molecules such as acetylcholine, gamma-aminobutyric acid (GABA) and glutamic acid is dependent on the tissue morphology.[179] In both cases, the matrix effects were compensated by the inclusion of an IS in the nano-DESI solvent which ionizes similarly as the analyte ions. As mentioned earlier, nanospray is not as sensitive to matrix effects compared to regular ESI due to the smaller initial droplets and thus, more efficient desolvation. This is also the case for the pneumatically assisted nano-DESI as the nebulizing gas improves the desolvation efficiency of the droplets and thus leading to reduced ionization suppression of metabolites.[69] Ion images of internal standards acetylcholine-d_9 and glutamine-$^{15}N_2$ spiked in the PA nano-DESI solvent did not show altered abundance in different regions of a mouse brain (**Figure 10**), thus, the PA nano-DESI is less affected by matrix effects compared to conventional nano-DESI.

To compensate for matrix effects during MSI analysis, the response of the analyte is divided by the response of the IS to obtain the normalized intensity. Importantly, the same adduct should be used for the analyte and the IS.[74,108] The choice of the standard is important for the correction of matrix effects. The optimal choice is a stable isotope-labelled version of the investigated analyte[105,115] since the physicochemical and ionization properties of such pair are very similar. However, a stable isotope-labelled version of the analyte is not always available or it becomes unpractical to include an IS for each analyte. In that regard, structurally similar compounds are an alternative. For example, Lanekoff *et al*. used two PC standards to account for matrix effects and quantify 22 endogenous PCs.[180] This approach enables calcula-

tion of the relative ionization of each phospholipid due to the acyl chain differences and was necessary for comparing quantities between different phospholipids. For relative comparisons, one standard can be used within the same molecular class. For example, in **Paper III** we showed that the ionization suppression between the C18-acylcarnitine-d_3 and carnitine-d_3 standards is not different between two important regions of the brain; the healthy and ischemic. In **Paper I** the detected concentrations of lysophosphatidylcholine (LPC) 18:1 was the same whether using the IS LPC 17:1 or LPC 13:0. To determine whether two compounds are differentially ionizing throughout a tissue section, their ratio is usually depicted. With this approach it was shown for example that the pairs PC 25:0 - PC 43:6, PGE_2-d_9 – PGF_{2a}-d_9 and carnitine-d_3 – C18-acylcarnitine-d_3 have similar ionization suppression throughout the tissue.[71,91,108]

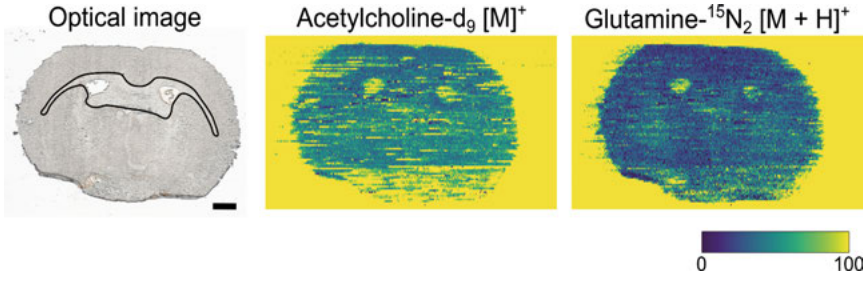

Figure 10. PA nano-DESI MSI of small molecules is not affected by the chemical environment. The optical image of the analyzed mouse brain tissue section shows the white matter region in black selection. Ionization of small molecules is different in this region compared to the rest (grey matter) (Bergman *et al.* 2016). PA nano-DESI MSI shows that acetylcholine-d_9 and glutamine-$^{15}N_2$ standards spiked in the solvent are not ionizing differentially throughout the tissue section. The signal outside the tissue area is higher due to ionization suppression from the tissue. Scale bar in the optical images shows 1 mm. The colormap scales goes from to 0 to 100% relative intensity and the contrast has been adjusted for clarity.

The use of carefully chosen standards is imperative for unbiased results during MSI. However, it is unpractical to include a standard for each analyte and further it requires knowing beforehand which analytes are of interest (targeted analysis). Besides the practical part of the problem, the effect of ionization efficiency should be considered. If too many standards are included then the risk of suppressing the ionization is big. These standards will also compete for surface position on the droplet surface during ESI. The answer to the question "*how much is too much?*" is not easy to obtain. In **Paper II** we pushed the limits by including up to 31 individual compounds as standards, the highest amount known up to date for nano-DESI MSI experiments. To assess whether

ionization suppression occurred due to the presence of the standards a systematic investigation is required. A comparison of signal intensities of endogenous molecules from tissue (ideally a mimetic tissue model to eliminate biological variation) with and without standards present could provide useful evidence. The ionization process during ESI is complicated by the fact that the presence of standards may alter the conductivity of the solvent and therefore affect the obtained signal intensity. Nonetheless, this is a topic of particular interest for future research.

In cases where non-targeted analysis is required, the inclusion of internal standards becomes a challenge. In this line of research, Kruve *et al.* has studied extensively the possibility of predicting ionization efficiencies and applying appropriate scale factors for non-targeted analysis.[181–184] In the discussion for quantitation in MSI the equation (1) used was introduced:

$$C_{end} = a \times \frac{I_{end}}{I_{std}} \times C_{std} \quad (1)$$

Therefore, knowledge of the response factor *a* between the endogenous compound and the standard used is a valuable piece of information for correcting their differential responses. At this point, it is worth mentioning that interpretation of data from non-targeted analysis is not straightforward, particularly in MSI where the benefit of a separation method is not present. Identification of analytes in MSI is a bottleneck that requires accurate mass, high resolving power, high quality MS/MS data and eventually the analysis of a pure standard for final confirmation. Usually, MSI data are complemented by an orthogonal method such as LC-MS, ion mobility (IM) or CE-MS (**Paper V**) for the analysis of tissue extracts or for surface sampling that allows higher confidence in the annotations.

Applications of (PA) nano-DESI MSI in ischemic stroke

Studying and understanding the mechanisms of ischemic stroke is vital for the development of treatments. While **Paper I** and **Paper III** are considered applications of MSI in ischemic stroke, several analytical observations are discussed. These were important for establishing a robust methodology. In **Paper I**, the administration of a neuroprotective agent, cytosine-guanine (CpG) oligodeoxynucleotides, was evaluated for protecting the ischemic brain. In **Paper III** the effect of ischemic stroke on the levels of acylcarnitines involved in mitochondrial fatty acid oxidation was investigated.

Alterations of phospholipids in preconditioned ischemic mice

Cell membrane disruption is characteristic of ischemic stroke[159] and thus, this study was focused on phospholipids, specifically, phosphatidylcholines (PCs) and lysophosphatidylcholines (LPCs). Several studies have shown that enzymatic degradation of PCs to LPCs occurs during ischemic stroke[185–187], therefore, LPCs are expected to accumulate in the ischemic area.

To accurately represent the accumulation of LPCs it was necessary to account for salt-related matrix effects in the ischemic area due to the imbalance of Na/K induced by the ischemic stroke. Accurate representation of ion images is essential for the reporting of chemical alterations. It was found that when TIC normalization, a common MSI data normalization method was used, the observations of endogenous LPC 18:1 were inconsistent. Since Na^+ is increased and K^+ is decreased in the ischemic region, LPC 18:1 appeared to accumulate at higher levels when detected as Na^+ adduct compared to K^+ adduct. This finding demonstrates that TIC normalization is not appropriate in cases of salt-related matrix effects. Further, several studies have shown that normalization to an IS is preferred over scaling factors for ion intensities.[116,117,188–193] However, isotopically labelled internal standards might not always be available for certain analytes. In such cases, the TEC normalization has shown to be effective for determining the extend of matrix effects on the target analyte.[109,110] Nonetheless, identification and compensation of matrix effects in MSI is necessary.

When the data were normalized to the corresponding adduct of the IS LPC 17:1, the change of endogenous LPC 18:1 was consistent among both alkali metal ion adducts. This was due to the similar adduct formation and ionization efficiency of the IS LPC 17:1 and the endogenous LPC 18:1 due to having the same cation binding site.[168] Thus, data normalization using the IS allowed for unbiased reporting of results. Further, it was demonstrated that LPC 13:0 and LPC 17:1 could be used interchangeably for normalizing data from endogenous LPCs. Due to the small differences in their structure, the ionization efficiency and hence the ionization suppression of these two ISs is similar but as the size of acyl chain increases, the suppression becomes less pronounced (**Figure 11**). The ionization suppression was calculated according to the following equation:

$$\%\, Suppresion = \frac{\left|I_{tissue} - I_{glass}\right|}{I_{glass}} x\ 100 \quad (2)$$

where I_{tissue} and I_{glass} are the mass spectrometric intensities of an *m/z* ion on tissue and glass, respectively. Overall, two important analytical observations were made: first, the use of appropriate internal standards is imperative for unbiased analysis and second, the use of structurally similar compounds for signal normalization is an effective method.[183]

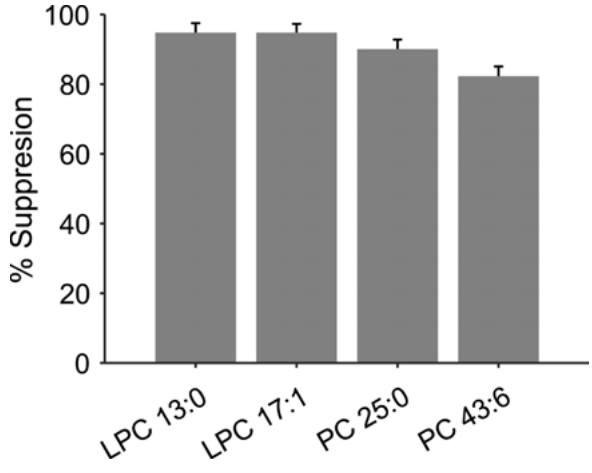

Figure 11. Ionization suppression for potassiated adducts of LPC 13:0, LPC 17:1, PC 25:0 and PC 43:6. Average ionization suppression and standard deviation were calculated from 4 consecutive line scans of an imaging dataset, according to the equation 2.

Using nano-DESI, ischemic mice brains were imaged with and without the administration of the preconditioning agent. Besides the visually reduced damaged ischemic area in preconditioned mice, various alterations in PCs and LPCs were observed. Mice that were not preconditioned with CpG demonstrated lower levels of PCs and higher levels of LPCs in the ischemic area compared to the healthy one. In preconditioned mice, no difference was observed regarding the PCs content between the healthy and ischemic areas, however, LPCs showed accumulation. The magnitude of LPCs accumulation in preconditioned mice was lower than non-preconditioned mice, indicating that the administration of CpG effectively protects the cell membranes by reducing the degradation of phospholipids. An important biological observation from this study is that CpG preconditioning does not seem to alter the chemical mechanisms induced during ischemic stroke, since CpG preconditioned mice still showed accumulation of LPCs. It is rather the extent of damage that is altered, which was confirmed both visually as well as molecularly.

Alterations of acylcarnitines in ischemic mice

Mitochondria are the energy factories of cells, producing ATP through oxidative phosphorylation. During ischemic stroke, the oxidative stress that is induced due to ionic imbalance and high levels of accumulated ADP are toxic for these organelles.[149] Therefore, energy production and mitochondrial dysfunction are associated in ischemic stroke. While β-oxidation is not as efficient and favorable in brain as oxidative phosphorylation and glycolysis, up to 20 % of the produced energy can occur through oxidation of fatty acids.[194] Oxidation of fatty acids requires their conversion to acylcarnitines through the carnitine shuttle system for transportation inside the mitochondria. Several reports have highlighted the importance of assessing the cell's energy status by measuring levels of acylcarnitines.[195–197] Therefore, the focus of this study was on the alterations of acylcarnitines after ischemic stroke.

Unbiased analysis in MSI requires careful consideration and compensation of matrix effects. The healthy and ischemic hemispheres are typically compared to each other for reporting chemical alterations (quantitative and qualitative), but the possible differences in the chemical environment[108,110] between those two regions had not been evaluated before. In this study, the suppression of two carnitine standards, carnitine-d_3 and C18-acylcarnitine-d_3 was compared between the healthy and ischemic region and was not found to be different. However, it was not possible to pinpoint whether this effect is due to the PA nano-DESI being less prone to matrix effects compared to conventional nano-DESI[69] (**Figure 12**) or due to the chemical environment being similar. Noteworthy, the suppression magnitude of carnitine-d_3 and C18-acylcarnitine-d_3 was slightly different, with the latter being suppressed ~12% more. This finding was unexpected since the structure-related effect on ionization efficiency is a well-known phenomenon.[184,198–201] Typically, more hydrophobic compounds exhibit higher ionization efficiency and therefore less ionization suppression which would be the case for C18-acylcarnitine-d_3 compared to carnitine-d_3, or PC 43:6 compared to PC 25:0 (**Figure 11**). However, we observed higher suppression for the more ionizable compound, C18-acylcarnitine-d_3 in our data. Scan-to-scan variation in this dataset was 17-24% which indicates that the ionization suppression difference is within the margin of error and thus not significant. Further, appropriate data normalization allowed the comparison of datasets that were acquired under slightly different conditions (solvent flow rate and concentration of standards). This observation highlights the robustness of the relative quantification in PA nano-DESI MSI using internal standards. Overall, structural analogs as internal standards were shown to be a robust option for the analysis of analytes within the same molecular class.

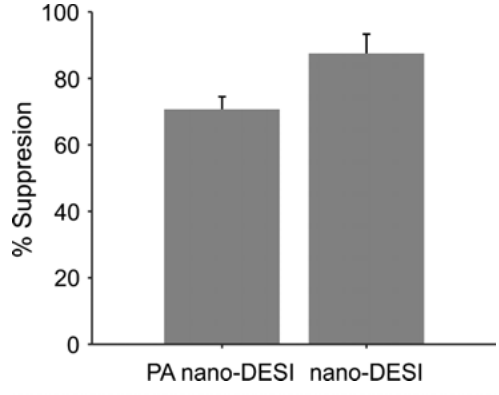

Figure 12. Comparison of ion suppression in PA nano-DESI (PC 25:0 standard) and nano-DESI (PC 22:0 standard). The average ionization suppression and standard deviation was calculated for 5 consecutive lines from imaging datasets using the potassiated adduct according to the equation 2.

Fragmentation studies of compounds of interest are important for structural elucidation and identification. Further, characteristic product ions can increase the selectivity and sensitivity of the analysis. In this study, we investigated the HCD fragmentation of carnitine-d_3 and C18-acylcarnitine-d_3, two molecules of the same class but with different acyl chain length. Noteworthy, those two molecules showed different fragmentation efficiencies which have important implications for analyses where selected reaction monitoring or multiple reaction monitoring is employed. Thus, even molecules of the same class should be optimized individually for MS/MS analysis to not compromise sensitivity while the fragmentation mode (*e.g.* CID or HCD) should also be considered.[202–204]

Imaging of the ischemic mouse brain using PA nano-DESI revealed that several long-chain (C14, C16, C18) acylcarnitines accumulated significantly in the ischemic region. The detection of individual acylcarnitines enabled the estimation of the activities for the main enzymes involved in the carnitine shuttle system, carnitine palmitoyltransferase 1 (CPT1) and carnitine palmitoyltransferase 2 (CPT2). The results showed that both CPT1 and CPT2 appear to have increased activities. However, the accumulation of long-chain acylcarnitines is most likely attributed to the much higher increased activity of CPT1, which is the rate limiting enzyme in the carnitine shuttle system. Further evidence of increased CPT1 activity include the lack of its natural inhibitor, malonyl-CoA and lack of accumulated free fatty acids in the ischemic region which are the substrates for CPT1. Even though it was not possible to

pinpoint the exact point that the carnitine shuttle system was disrupted, our data provide clear evidence for the obstruction of mitochondrial β-oxidation. While our MSI analysis of acylcarnitines in ischemic stroke provides evidence for disturbed metabolic pathways, complimentary data are required for obtaining a comprehensive view of the underlying mechanisms. Future work of assessing individual enzymatic activities of the enzymes involved in the carnitine shuttle system would provide further evidence in the assessment of the status of β-oxidation. Finally, this work demonstrated the high degree of localization of long-chain acylcarnitines in the ischemic area which would not be possible to decipher with traditional bulk analysis.

Development of analytical methods

Determination of Na^+ and K^+ using host-guest chemistry

Sodium and potassium ions are important alkali metal ions contributing to the ionic balance of cells. Further, their intracellular and extracellular concentrations are tightly regulated by the Na/K ATPase. Ionic imbalances caused by diseases can severely affect the homeostasis of the cells, as is in the case of ischemic stroke. Therefore, analytical methods that determine alkali metal ions in biological systems are relevant. While there are numerous methods for elemental determination both with and without spatial information[205–208], the simultaneous determination of elemental and molecular distributions has not been explored extensively.[209] Simultaneous determination of alkali metal ions and molecules is advantageous since it increases the throughput of the analytical method by requiring fewer samples and less analysis time. Modern high resolution mass spectrometers (> 100000 resolving power at *m/z* below 400) are not capable of scanning at *m/z* below 50, therefore, direct measurement of light alkali metal ions such as Na^+ (*m/z* 22.98922) and K^+ (*m/z* 38.96316) is impossible. In **Paper II** we showed that indirect determination is possible using host-guest chemistry with crown ethers.

Crown ethers are macroheterocyclic compounds that have found extensive use as phase transfer catalysts for bringing ionic species in environments that they typically would not be found *e.g.* hydrophobic phases.[210] Their complexation properties with alkali metal ions is related to their structure.[211,212] We chose to develop a method based on crown ethers since they are inexpensive, easy to obtain, their different structures allow for fine-tuning of the complexation for the individual alkali metal ions and they also have high ionization efficiencies. Complexation of individual alkali metal ions with crown ethers is not a linear process, unless the binding affinities for each alkali metal ion are of similar magnitude (**Figure 13**). It should be noted that a high value of binding affinity yields larger number of formed complexes but

the saturation of the complexation is realized at lower concentrations. However, it was observed that by using the intensity ratio of the two crown ether complexes, a linear response can be obtained throughout the alkali metal ions concentration ratio range (**Figure 13**). Additionally, using the intensity ratio had several further advantages: the response is unaffected by the total concentration of the guests (*i.e.* Na^+ and K^+), unaffected by the host (*i.e.* crown ether) concentration and unaffected by the matrix effects during ESI. Since the intensity ratio of $[crown\ ether + Na]^+/[crown\ ether + K]^+$ is used throughout the

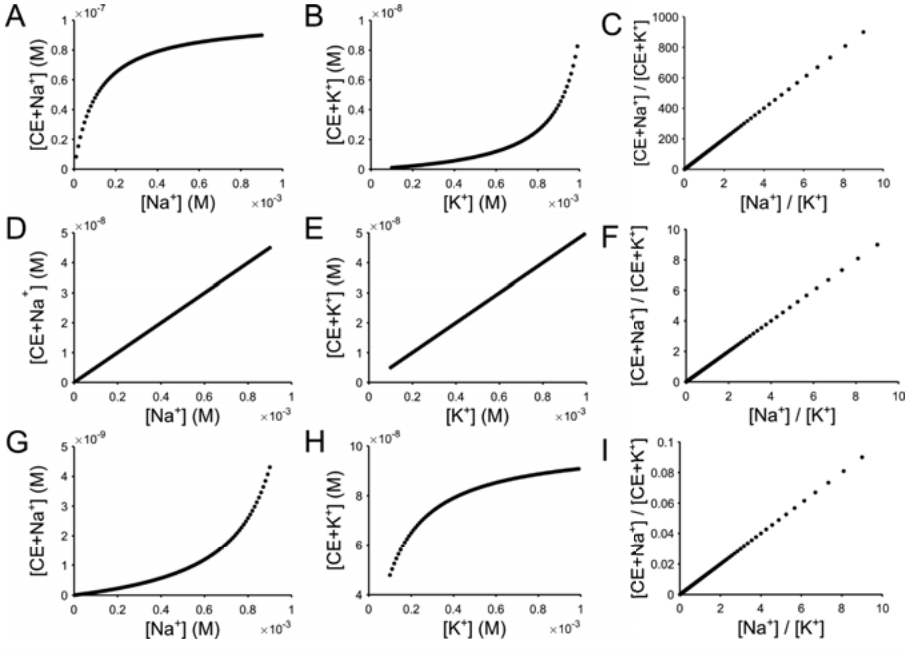

Figure 13. Calculated equilibrium concentrations of a hypothetical crown ether (CE) and Na^+ or K^+ at various proportions of Na and K ions. The total concentration of alkali metal ions remains constant (1 mM) while their relative proportions change. Data were obtained by solving simultaneous equilibrium equations (Supporting information of **Paper II**) where the crown ether concentration is fixed at 0.1 µM. A-C) A crown ether with $\log(Kb_{Na}) = 4$ and $\log(Kb_K) = 2$. D-F) A crown ether with $\log(Kb_{Na}) = 3$ and $\log(Kb_K) = 3$. G-I) A crown ether with $\log(Kb_{Na}) = 2$ and $\log(Kb_K) = 4$.

method, it would be reasonable to assume that any molecule that forms sodiated and potassiated adducts *e.g.* a phospholipid IS could be used instead of crown ethers. However, our selected host molecule should preferably form complexes with Na^+ and K^+ ions, so the presence of protonated adducts is not desired as changes in the pH of the sample would influence the complexation process. This was also taken into account during the crown ether selection process, resulting in the final candidate, dibenzo-18-crown-6 as the most suitable, among those studied.

The developed method was applied to PA nano-DESI MSI of ischemic mouse brain where Na^+ and K^+ alterations are expected in the ischemic region. Due to high ionization efficiency, the selected crown ether was spiked at low concentration (0.1 μM) directly in the sampling solvent. The amount of Na^+ and K^+ present in biological systems is typically in the order of mM, which means that the complexation process does not use all available alkali metal ions. However, this is not a limitation since monitoring the intensity ratio of the two crown ether complexes provides a measurement of the $[Na^+]/[K^+]$ regardless of the total amount of sodium and potassium ions present. By using a simple offline calibration curve of intensity ratio versus $[Na^+]/[K^+]$, the intensity ratio of crown ether complexes obtained from the tissue section during MSI can be directly converted to $[Na^+]/[K^+]$. To obtain individual abundances of alkali metal ions, another offline calibration curve using a mimetic tissue model spiked with Na^+ was used to obtain the concentration of Na^+. At the same time, the molecular information obtained during a PA nano-DESI MSI experiment is readily obtained at no analytical cost. Overall, the developed method allowed for obtaining abundances of alkali metal ions Na and K directly from tissue sections by simply adding crown ethers in the PA nano-DESI solvent.

Determination of prostaglandin isomers using tandem MS and silver cationization

The presence of isomers and isobars in mass spectrometry constitutes a major bottleneck in the identification of molecular ions. Isobars have the same nominal mass but different exact masses, therefore, high resolution mass spectrometers can separate them by *m/z*, up to a certain extent. On the other hand, isomers have the same chemical formula, thus, the same exact mass but different structure. For instance, prostaglandins (PGs) are important lipid mediators that are involved in physiological processes where the various isomers can have opposing effects.[213,214] Among the PGs molecular class, various isomers share the same chemical formula; $C_{20}H_{32}O_5$. Thus, separation based on *m/z* is not possible. To tackle that, separations based on physicochemical properties of the compounds are employed. For example, chromatography and capillary electrophoresis are among the most used methods for separating isomers.[215] However, such methods are not capable of providing spatial information due to the vastly different time scales of MSI experiments and separation. For that, ion mobility has shown that it can be coupled with MSI techniques for separation of isomers based on their mobility.[85,216–220] Another interesting approach for distinguishing isomers is the use of tandem mass spectrometry[221] which is compatible with MSI and requires little to no instrument modification. In **Paper IV** a methodology based on tandem MS was developed to distinguish biologically relevant isomers of prostaglandins.

Analysis of PGs is typically done in the negative ion mode where they are detected as deprotonated ions.[222–224] Tandem MS of PGs in the negative ion mode has been extensively studied[225,226] but it has not been demonstrated so far that the fragmentation provides informative product ions that can aid in distinguishing the different isomers. Further, it has been previously shown that incorporation of silver ions (Ag^+) in the nano-DESI solvent vastly increases the sensitivity for detecting PGs as silver adducts, compared to deprotonated ions[91], which is desired due to their inherently low abundances. In this work, the use of Ag^+ was pivotal for the developed method since product ions originating from specific isomers were identified. Even though PGs with the chemical formula $C_{20}H_{32}O_5$ can include many isomers, we have narrowed down our study to the most stable and biologically important, PGE_2, PGD_2 and Δ12-PGD_2. Tandem MS of the three isomers cationized with Ag^+ demonstrated that characteristic product ions can be identified originating from PGE_2 (*m/z* 331.0096) and Δ12-PGD_2 (*m/z* 341.0301) using MS^3. Further, all three isomers have a common product ion (*m/z* 333.2060) resulting from the loss of silver hydride, AgH, in MS^3 level, at different abundances due to their different structures. The observation that the relative abundances of these three product ions were different between the isomers was the basis for the development of prediction models, as has been demonstrated before for phospholipids, fatty acids and peptides.[73,88,90,93,227] During the final selection of the product ions for training the prediction models, LC-MS analysis of a chemically complex sample (rat brain extract) provided useful information on the uniqueness of the formed product ions (**Figure 14**). Given the inherent limitations of ion traps and quadrupoles for selecting precursors with a narrow isolation window, isobaric compounds that give rise to product ions with the same *m/z* would contaminate the spectra and produce erroneous results.

The prediction models were trained using data acquired from a unit mass resolution linear ion trap instead of the high resolution orbitrap. There are several advantages in using an ion trap: speed, sensitivity and increased signal-to-noise ratio.[228] All the above are contributing to detecting product ions from low abundance PGs in MS^3 level. Therefore, it was possible to train robust and accurate prediction models that were directly applicable to PA nano-DESI MSI data from biological tissue sections. The developed method was used to identify which PG isomers present in a tissue section from a mouse embryo implantation site and their localization. All three product ions used for the prediction models were detected and used for predicting the relative abundance of each isomer. We found distinct localization of all three isomers in the anti-mesometrial pole of the implantation site and the luminal epithelium but with different abundances for each isomer. Δ12-PGD_2, a degradation product of PGD_2 was detected with the highest abundance. This was not unexpected due to the long storage of the tissue section in the freezer. PGE_2 was the second most abundant isomer and finally PGD_2 was the least

abundant. These results demonstrated for the first time, isomeric imaging of major PG isomers without any instrumental modification.

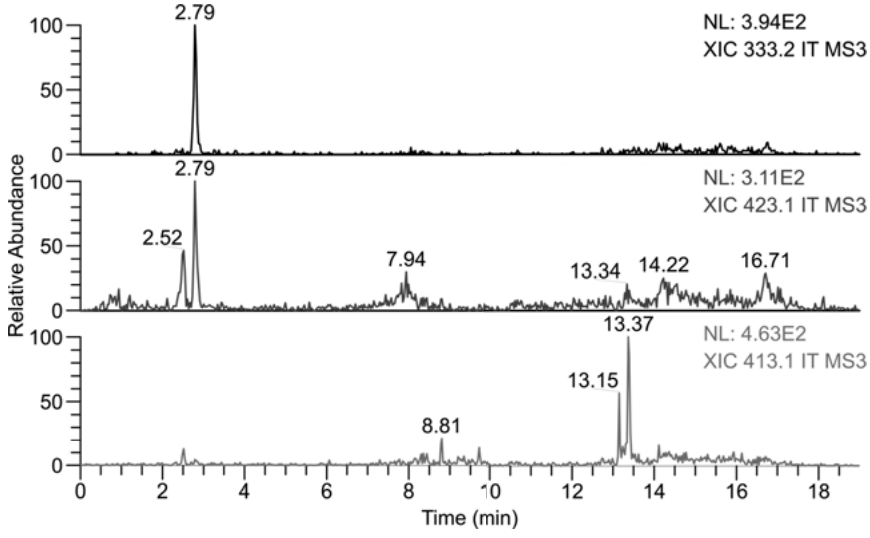

Figure 14. LC-MS^3 with post-column addition of Ag^+ from a chemically complex sample (rat brain extract) where various extracted ion chromatograms (XICs) are shown. The MS^3 transition *m/z* 459.13 → 441.12 was selected. PGE_2 elutes at 2.52 min while PGD_2 at 2.79 min. The product ion *m/z* 333.2 is produced mainly from PGD2 (top panel). The product ion *m/z* 423.1 is produced by both PGE_2 and PGD_2 but also from other isobars (middle panel). The product ion *m/z* 413.1 is produced mainly by isobars (bottom panel).

Beyond the *m/z* in MSI: combination with SS-CE-MS for confident molecular annotations

Another approach to tackle the presence of isomers and isobars in mass spectrometry is separation. Previous studies have demonstrated that molecules can be sampled directly from tissue sections and introduced in an LC-MS system for separation and subsequent mass spectrometric detection.[229] Apart from isomer separation, enhanced sensitivity of analytes can be realized due to the reduced matrix effects. Developments in SS-CE-MS[142,143], previously shown by our research group, have established this technique as a great complementary tool for separating molecules that are sampled directly from tissue sections. While CE-MS systems are commercially available (*e.g.* Agilent® 7100 CE which can be coupled with any Agilent® LC-MS system), SS-CE-MS is still undergoing developments to increase its robustness and

user-friendliness. In **Paper V** we have combined the best of two worlds: visualization of molecular distributions through PA nano-DESI MSI and separation of isomers with CE-MS.

The aim of this work was to develop a workflow that uses a single tissue section and the same platform for both techniques. This was important for higher throughput and most importantly, direct correlation of the information obtained from MSI and SS-CE-MS. Key to this development was the design and 3D printing of holders that can accommodate different sampling probes. The schematic in **Figure 15** demonstrates the steps taken for analysis with PA nano-DESI MSI and SS-CE-MS. We use only two probe holders, one for the PA nano-DESI probe or the SS-CE emitter and one for the SS-CE sampling. After the MSI analysis is completed, the data are visualized through a custom-made application and specific locations from the tissue section can be selected for sampling with SS-CE-MS. This workflow allows for direct sampling from the analyzed tissue section with SS-CE-MS without the need for a new sample. Therefore, potentially interesting locations that are not visible in the bright field images but visible through molecular distributions, can be easily found and sampled.

The workflow uses one single tissue section that initially is analyzed by PA nano-DESI MSI and then sampled with SS-CE-MS. Therefore, the question of analyte depletion was relevant. Non-exhaustive sampling with nano-DESI MSI has been demonstrated before by Duncan *et al*.[230] Two individual tissue sections were analyzed with SS-CE-MS; one was previously imaged with PA nano-DESI MSI while the other was intact. Our analysis showed that analyte depletion was not significant and thus, analyte material was present for SS-CE-MS analysis after MSI. This finding was important for establishing the workflow of the technique. Further, the comparison of the information obtained from the techniques demonstrated the importance of the solvent. In PA nano-DESI MSI, both metabolites and lipids can be sampled while in SS-CE-MS, mainly polar metabolites due to the choice of sampling solvent. Golubova *et al*. has demonstrated that lipids can be sampled with SS-CE-MS by modifying the sampling solvent.[143] While the data from PA nano-DESI MSI provided larger metabolite coverage, isomeric separation was not possible. However, with SS-CE-MS from an imaged tissue section we confirmed the presence of both valine and betaine at the mass channel *m/z* 118.0864 at appreciable intensities. The presence of both compounds has hindered previous reports from confident annotation.[231,232] Furthermore, the mass channel *m/z* 90.0551 which is typically annotated as alanine[233–235] was found to contain three peaks. After analysis of standards it was concluded that these peaks corresponded to β-alanine, α-alanine and an in-source fragment of creatine. The complementary nature of this workflow is important for in-depth understanding of biological mechanisms in health and disease, and we have demonstrated that such characterization can be realized through one analytical platform.

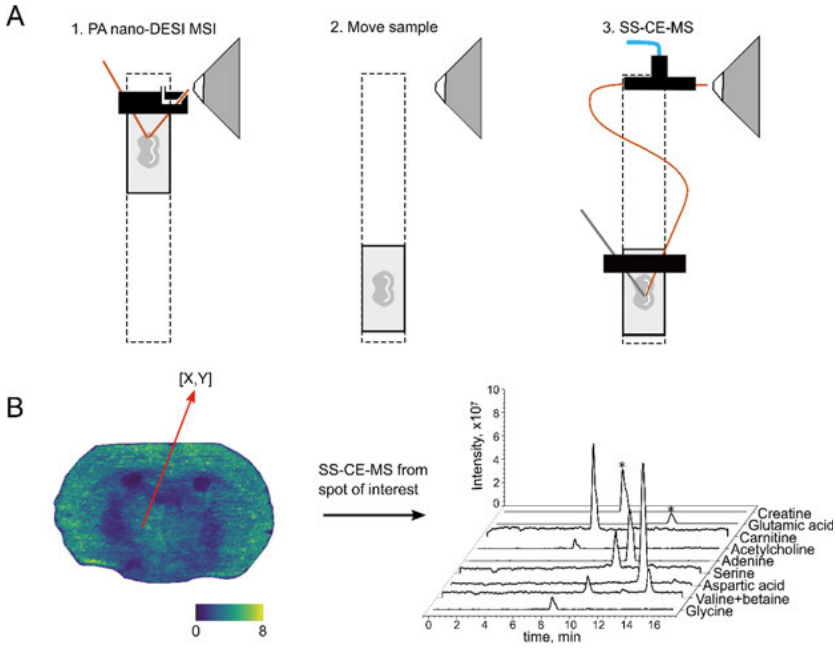

Figure 15. Schematic of the experimental workflow for combined imaging and SS-CE-MS analysis. A) A tissue section is analyzed first using PA nano-DESI MSI. After the analysis is completed, the sample is moved to an appropriate position for SS-CE-MS. B) Ion image of glutamic acid ([M – $H^+ + Na^+ + K^+$]) normalized to glutamic acid-d_3 (same adduct). Extracted electropherograms for various *m/z* channels of protonated ions putatively identified as glycine, adenine, aspartic acid, serine, valine/betaine, acetylcholine, carnitine, creatine and glutamic acid. The electropherograms were smoothed using a boxcar algorithm with 7 points. *For better presentation the intensity of creatine and glutamic acid was reduced by a factor of 50.

Conclusions and future perspectives

The scope of this thesis had dual nature: to showcase that MSI is a valuable tool for understanding chemical mechanisms in stroke and to develop novel analytical methodologies for challenging analytes. The former was achieved in **Paper I** and **III**. In **Paper I**, we showed that preconditioning with CpG oligodeoxynucleotides alleviated the ischemic damage as shown by the membrane lipid degradation. This finding is important for deeper understanding of the mechanisms behind ischemic preconditioning and for the development of neuroprotective agents. In **Paper III**, we used MSI to reveal disruptions in the carnitine shuttle system, a system that is important for the transportation of activated fatty acids into the mitochondria for β-oxidation to produce energy. Such findings aid in understanding how the brain utilizes energy during an ischemic stroke event. In both studies, it was evident that MSI alone cannot provide all necessary evidence, and thus, combination with other modalities *e.g.*, immunoassays, enzymatic studies, is necessary for deep understanding of disease.

In **Paper II**, **IV**, and **V** we demonstrate novel analytical methodologies for challenging analytes. Such analytes include alkali metal ions and isomers. In **Paper II** a method based on host-guest chemistry with crown ethers was developed for the determination of Na^+ and K^+ changes in MSI workflows simultaneously with molecular distributions of metabolites and lipids. Such method was valuable when using high resolution mass spectrometers that cannot scan below *m/z* 50 and thus direct determination of light alkali metal ions is impossible. In **Paper IV** a tandem MS method was developed for distinguishing prostaglandin isomers using Ag^+ cationization. The combination of silver cationization for increased ionization efficiency of prostaglandins and the detection of characteristic product ions from such adducts was key for developing a predictive model. In both **Paper II** and **IV**, the developed methodologies required only the addition of the appropriate dopants (crown ether or silver ions) in the PA nano-DESI solvent and no additional instrumental modification. In **Paper V** two analytical platforms, MSI and SS-CE-MS were combined in one to obtain both imaging and deep chemical characterization of metabolites. This was important for elucidating the presence of isomers in mass channels that with MSI alone cannot be resolved. In all studies, the analytical methodologies were extensively tested for robustness and relevance with biological samples, demonstrating their utility.

The present methods and applications add to the portfolio of MSI workflows. In all results presented, the tunability of the solvent in nano-DESI was key to either compensating for matrix effects or introducing dopants for interactions with analytes. Some unpublished results were presented in an effort to understand the extraction processes of the various solvents that can be used with nano-DESI MSI. Further understanding of this property can extend the current capabilities of the technique.

Matrix effects and signal normalization is a topic of utmost importance in MSI. Here, normalization is achieved by using isotopically labelled internal standards or structural analogs to the target analytes. However, in the future, developments in the field of non-targeted analysis could drive innovations in MSI as well. At this point, a bottleneck in MSI is that stable isotopes are not available for all compounds and, also, it is not practical to include a standard for each analyte, particularly in cases where hundreds of targets are of interest. Normalization approaches such as TIC are convenient and readily applicable but in certain cases, *e.g.* when alkali metal ions changes are contributing to the matrix effects, misleading results are obtained. Thus, more robust normalization methodologies need to be developed. The use of one standard for a plethora of analytes within the same molecular class is promising and understanding how relative ionization efficiencies can be utilized is needed for robust normalization.

Quantitation is also a bottleneck in MSI workflows. Noteworthy, this is related to the lack of appropriate standards for each of the analytes that are to be quantified as well appropriate tissue models that mimic the actual tissue environment. Tissue homogenates spiked with appropriate standards can be used, but the tissue environment is not as heterogeneous as the native tissue. Nonetheless, this is the best option so far. In all MSI analyses, deep understanding of matrix effects is necessary for the development of robust quantitative methods. Further, the extraction efficiency of the analytes is difficult to determine and thus, absolute quantitation is rarely realized. Understanding the extraction efficiency of analytes from tissue would open new avenues for quantitative MSI. Hopefully, further developments will drive the field towards robust quantitative workflows.

Mass spectrometry imaging is an impactful field within mass spectrometric workflows. Constant analytical developments in spatial resolution, ionization efficiency, matrix effects compensation, normalization, quantitation and resolving isomeric species are pushing the boundaries of the field and reveal exciting applications in understanding molecular mechanisms in metabolism. Further, technological developments in mass spectrometers are extending the capabilities of MSI workflows. In the future, standardization of MSI and utilization in clinical applications will be one of the highlights of the field.

Popular scientific summary

Approximately 30 000 people suffer from stroke every year in Sweden. Ischemic stroke occurs when the blood flow towards an organ (*e.g.* brain) is obstructed. It is the most common form of stroke and one of the leading causes of death and disability in the world. Therefore it is important to understand ischemic stroke to develop treatments. Understanding metabolism (the process of converting food to energy) and disease is the topic of bioanalytical chemistry. However, understanding the role of molecules in disease is not easy because some important molecules are difficult to analyze. Thus, we need to develop new methods to reach that goal. In my thesis I have developed analytical methods for molecules that are challenging. Additionally, I have applied analytical methodologies to understand and reveal mechanisms of ischemic stroke in brain. This was achieved by using mass spectrometry imaging which can provide information on the identity, quantity and localization of molecules in a biological sample.

Probably the most known imaging method is magnetic resonance imaging which uses a strong magnet to visualize density changes in our body. However, to visualize the chemical distribution in tissue, imaging needs to be coupled to a mass spectrometer that can provide information about charged molecules or atoms, *i.e.* ions, based on their mass-to-charge ratio. With mass spectrometry imaging various samples can be analyzed: sections from healthy tissue or biopsies. This allows for direct localization of the molecules of interest on the tissue section and for relating this information to disease occurrence or progression. In this thesis I have used a technique called nano-DESI that uses a liquid flow to "transfer" molecules from a distinct location on the tissue section to the mass spectrometer for analysis.

Sometimes we handle stressful situations better if we have been previously exposed to a similar event. Likewise, our brain can defend itself better against ischemic stroke if it has been prepared for it, a method known as preconditioning. For example, preconditioning can be achieved by having a small and harmless incident of stroke so that the brain builds defense mechanisms. It can also be achieved by the use of chemical agents. In **Paper I,** I studied the effect of a preconditioning agent, CpG oligodeoxynucleotides, given to mice before having ischemic stroke. The results showed that the damage was reduced in the brain of mice that were treated with CpG before the stroke. This was re-

vealed by looking at the degradation of specific components of the cell's protection shell, phospholipids. Therefore, treatment with CpG was effective at reducing the damage caused by stroke.

Our brain requires a lot of energy to complete the complicated tasks of everyday life. Typically, the energy is taken from glucose, which is found in sugar but fatty acids can also provide fuel for the brain. Fatty acids are part of fat which our body breaks down to generate energy. During ischemic stroke the brain is literally starved from glucose and oxygen which leads to damage of brain cells. In **Paper III**, I studied the effect of ischemic stroke on the metabolism of fatty acids for energy usage. Fatty acids themselves cannot enter the cells so they have to be transported. This is achieved when they are connected to carnitine, forming acylcarnitines. Once these are in the cell, the carnitine is released and the fatty acids can be used for energy production. We found that after ischemic stroke the fatty acids were trapped in the form of acylcarnitines and could not be released to produce energy. Therefore, the brain was not able to use fatty acids to survive the ischemic stroke.

In bioanalysis, molecules sometimes "play" hide and seek and they are very good at it. Thus, the researchers try to develop new analytical methods to determine these molecules. In **Paper II**, I studied the changes of sodium and potassium in brain after ischemic stroke. Sodium and potassium are important markers for the well-being of cells. Unfortunately, the mass spectrometer is "blind" to their presence because of their light mass. However, we were able to form a new molecule by using cyclic chemical compounds (crown ethers) that include the sodium and potassium ions. Now the new molecules are heavier and detectable by the mass spectrometer!

In **Paper IV**, our target molecules were prostaglandins present in the embryo implantation site of pregnant mice. Prostaglandins are important molecules involved in pain and pregnancy but they are difficult to analyze. They come in many different shapes and forms but with the same mass, called isomers. This makes it difficult for the mass spectrometer to tell them apart. When they interact with silver ions they form a new molecule. The new molecules, depending on the isomer form of prostaglandin, will behave differently when we apply energy to break them down in smaller pieces. Now we are able to tell them apart!

In **Paper V**, the problem of the isomers was tackled from a different angle. Here, instead of forming a new molecule, we used a complimentary technique that can separate the isomers. This technique, called surface sampling capillary electrophoresis, uses very high voltage to separate ions. Being able to understand which isomer contributes to the information that we obtain is important for fully understanding chemical mechanisms of life.

Populärvetenskaplig sammanfattning

Ungefär 30 000 personer drabbas av stroke i Sverige varje år. Ischemisk stroke inträffar då blodtillförseln till ett organ (t.ex. hjärnan) är blockerad. Ischemisk stroke är den vanligaste formen av stroke och är en av de ledande orsakerna till död och invaliditet. För att utveckla behandlingar är det viktigt att förstå hur ischemisk stroke fungerar. En gren inom bioanalytisk kemi är att studera sjukdomstillståndens metabolism (vilket exempelvis är processen som ger oss energi från maten) för att få nya insikter om sjukdomar. Det är dock inte alltid enkelt att studera specifika molekylers roll vid sjukdomstillstånd då många viktiga molekyler kan vara svåra att mäta. Därför behövs det nya analytiska metoder, så att man kan mäta så mycket som möjligt. I min avhandling har jag utvecklat nya metoder för att kunna mäta och förstå metabolism i biologiska system. Specifikt så har jag använt avbildande masspektrometri för att bestämma molekylers identitet, kvantitet och placering i vävnad.

I dagsläget är magnetröntgen den mest välkända metoden för avbildning av vävnad. Men för att kunna visualisera kemin i vävnad krävs det att avbildningstekniken är kopplad till en masspektrometer. En masspektrometer ger information om vilka laddade molekyler eller atomer, s.k. joner, som finns i provet genom att mäta deras förhållande mellan massa och laddning. Med avbildande masspektrometri kan man därmed visualisera var i vävnaden molekylerna finns. Exempelvis kan frisk vävnad analyseras för att få en bild av kemin i ett friskt prov, vilket sedan kan jämföras med kemin i ett vävnadsområde som drabbats av ett sjukdomstillstånd för att förstå hur metabolismen ändrats. I denna avhandling har jag använt en avbildningsteknik som kallas nano-DESI. Denna teknik använder ett lösningsmedel för att transportera molekylerna från en distinkt position på vävnadens yta till masspektrometern för analys.

Ibland hanterar vi en stressig händelse bättre om vi tidigare har blivit utsatta för en liknande situation. På samma sätt så kan hjärnan försvara sig bättre mot en ischemisk stroke om den är förberedd, en metod som kallas prekonditionering. Detta kan uppnås genom exponering för korta och ofarliga ischemiska händelser. Det kan också nås genom kemisk behandling, t.ex. med CpG oligodeoxynukleotider. I **Paper I** har jag studerat hur CpG behandlade möss påverkas av ischemisk stroke. Jag upptäckte en lägre grad av degradering av fosfolipider vilket betyder att de CpG behandlade mössen hade mindre skada

i hjärnan efter stroke. Behandling med CpG innan stroke kan därför ses som ett alternativt sätt att minska skador i hjärnan från ischemisk stroke.

Vår hjärna är ett mycket komplex organ som kräver mycket energi för att fungera. Hjärnan får vanligtvis energi från metabolism av glukos som finns i socker, men fettsyror kan också används som energikälla. Fettsyror är byggstenar av fett som vår kropp används som bränsle. Under ischemisk stroke får hjärnan ingen glukos och syre på grund av att blodtillförseln är blockerad. I **Paper III** studerade jag hur ischemisk stroke påverkar metabolismen av fettsyror i hjärnan. För att fettsyror skall kunna ge energi i cellen måste de först kopplas till en molekyl som heter karnitin, och bilda acylkarnitin. När acylkarnitin har transporterats till rätt ställe i cellen så avlägsnas karnitin och fettsyran kan då använts för energiproduktion. Med avbildande masspektrometri visade jag att acylkarnitiner inte omvandlades tillbaka till fettsyror i ischemisk stroke, och kan därmed inte användas som bränsle i hjärnan.

I bioanalys ”leker” molekylerna ibland kurragömma och de är ganska duktiga på det! Därför behöver forskare utveckla nya analytiska metoder för att hitta fler olika molekyler. I **Paper II** var syftet att visualisera förändringar av natrium och kalium i hjärnan efter ischemisk stroke. Dessa atomer är mycket viktiga hälsomarkörer för cellerna. Tyvärr kan inte alla masspektrometrar ”se” natrium och kalium joner på grund av deras låga massa. Men genom att koppla dem till cykliska molekyler (kronetrar) bildas nya tyngre molekyler som kan analyseras med masspektrometri!

I **Paper IV** var målet att mäta prostaglandiner i livmodervävnad hos gravida möss. Prostaglandiner är viktiga ämnen som spelar stor roll i smärta och graviditet men som är svåra att analysera med masspektrometri. Svårigheten beror på att det finns många olika former av prostaglandiner som har samma massa, vilket kallas isomeri. Genom att koppla silver på prostaglandin isomererna och bryta ned de laddade molekylerna i mindre bitar i masspektrometern upptäckte jag att de faktiskt kunde särskiljas. Nu var det möjligt att separera dem!

I **Paper V** löstes problemet med isomerer på ett annat sätt. Här använde jag en annan teknik för att separera isomerer istället att bilda nya molekylerna som tidigare. Tekniken kallas kapillärelektrofores och där används en hög spänning för att separera joner på grund av deras olika form och storlek. Förståelse av vilken isomer bidrar till information som vi får från analysen är mycket viktigt för att få alla pusselbitar på plats, och få ihop en hel bild av sjukdomars kemiska mekanismer.

Acknowledgements

First and foremost, I am eternally thankful to my parents. I cannot express enough my gratitude and love for your unconditional support throughout my studies. Your guidance and advice has shaped me up to today. Without you I would not be here. This thesis is dedicated to my late Grandpa, with whom I share more than my name, and was always proud and happy to see his grandchildren excel.

Μαμά, Μπαμπά, σας ευχαριστώ για όλα όσα έχετε κάνει για εμένα και την Δέσποινα. Δεν υπάρχουν λόγια να εκφράσω πόσο εκτιμώ την υποστήριξή σας όλα αυτά τα χρόνια. Χωρίς εσάς δεν θα ήμουν εδώ. Σας αγαπάω και μου λείπετε.

The second biggest acknowledgement is devoted to my PhD supervisor. **Ingela**, thank you for giving me the opportunity to undertake my PhD in Uppsala. I will always remember the moment at the airport the day after the interview when I read your email with the position offer. The coffee I had on the airplane some hours later was probably the most "happy" coffee I have had so far. Also, thank you for introducing me in all the Swedish traditions (kräftskivor, snaps, västerbottensostpaj, helan går) and for always including a social aspect in our group activities. I appreciate the trust you showed towards me and thank you for shaping my scientific career.

To past and current group members: **Kyle**, **Johan**, **Cátia**, **Varun**, **Gàbor**, **Felix**, **Eszter**, **Lucie**, **Nastia,** thank you for the great atmosphere in the lab, in the corridor, in the spray bar, in the office and outside BMC. It was always a pleasure to hear your thoughts and critique during group meetings and learn from each other. **Kyle**, you are the most enthusiastic researcher I know and your enthusiasm about projects and results was contagious. Thank you for your guidance during my first years as a PhD student! I wish you the best for your career! **Johan**, our office silliness was much needed to alleviate stress and frustration during tough lab times. Thank you for discgolf, Swedish humor and podcasts, Sirius matches and for challenging my scientific hypotheses. I will never forget you encouraging me to try bäska droppar (= bitter droplets, literally). **Cátia**, thank you for being a good friend and for your never-ending positivity. Don't forget to breathe. You might be one against many single cells, but you are on top of it! **Varun**, I admire your ability to memorize all the steroid isomers and recall them during group meetings. Keep up the good work! **Gàbor** (a.k.a. **Csongor**), thank you for bringing a mature perspective

into the lab for the past two years. Your input and feedback were always appreciated! You are a true beef boy. **Felix**, keep up "infecting" people around you with the gym bug! **Eszter S.**, I appreciate the calm and happy energy you bring to the lab and I'm sorry for all the times Johan and I tried to convince you about some silly non-true facts. **Lucie**, hej hej! It was great to have another person in the corridor that is into volleyball. **Cátia, Varun, Felix, Eszter S.** and **Lucie**, **Nastia,** best of luck with the rest of your PhD!

Ioanna, **Vlad**, **Weifeng**, **Carina**, **Sydney**, **Fan**, thank you for all the fun times at the spray bar, during lunch and outside of BMC! **Ioanna**, the third best cornhole player I know, I wish you the best for the rest of your PhD! It was nice to have another Greek in the corridor, so I don't forget my native language. **Vlad**, the ultimate table tennis opponent, and hiking companion up in the snowy mountains. I wish you a strong finish your PhD! **Weifeing**, tjena tjena. You are the most hardworking person I have met. Your PhD defense is going to be awesome! **Sydney**, what you sayin? Can't remember how many times we argued whether fresh or microwaved fries are better. Wish you the best for the rest of your PhD! **Carina** and **Fan**, thanks for the fun times during the Analytical Chemistry social events! **Sandy**, **Mark**, **Kumari**, **Anna**, thank you for the fun times during potluck dinners. **Farshid**, your help was always appreciated when instruments were not functioning during teaching times.

Maxim, we might not have started the fire, but we definitely had fun skiing and hiking together. I wish you and **Sarah** the best and I will miss our beer pong tournaments. **Eszter K.**, thanks for being the receiver of my sarcasm. I wish you the best for the future!

Daniel, thank you for being my co-supervisor. I always appreciated feedback from you. **Jeff**, thanks for all fruitful scientific and non-scientific related discussions. **Per**, tack för att du har varit en utmärkt kursledare och för ditt tålamod med mitt svenska uttal! **Jonas**, thanks for being there for us as a FUAP and for providing guidance during our studies!

Johanna, my little patootaki, thank you for all your support and for helping me develop as a person and as a partner. Thank you for being both my friend and my partner. I am looking forward to the future with you.

References

1. Gerlich, D. Inhomogeneous RF Fields: A Versatile Tool for the Study of Processes with Slow Ions. In *Advances in Chemical Physics*; Advances in Chemical Physics; 1992; pp. 1–176 ISBN 9780470141397.
2. Hamers, E.A.G.; van Sark, W.G.J.H.M.; Bezemer, J.; Goedheer, W.J.; van der Weg, W.F. On the Transmission Function of an Ion-Energy and Mass Spectrometer. *Int. J. Mass Spectrom. Ion Process.* **1998**, *173*, 91–98.
3. Wollnik, H. Ion Optics in Mass Spectrometers. *J. Mass Spectrom.* **1999**, *34*, 991–1006.
4. Kelly, R.T.; Tolmachev, A. V; Page, J.S.; Tang, K.; Smith, R.D. The Ion Funnel: Theory, Implementations, and Applications. *Mass Spectrom. Rev.* **2010**, *29*, 294–312.
5. De Hoffmann, E.; Stroobant, V. *Mass Spectrometry*; 3rd ed.; Wiley-Blackwell: Hoboken, NJ, 2007; ISBN 9780470033104.
6. Recommendations for Symbolism and Nomenclature for Mass Spectroscopy. *Pure Appl. Chem.* **1978**, *50*, 65–74.
7. Douglas, D.J. Linear Quadrupoles in Mass Spectrometry. *Mass Spectrom. Rev.* **2009**, *28*, 937–960.
8. Glish, G.L.; Vachet, R.W. The Basics of Mass Spectrometry in the Twenty-First Century. *Nat. Rev. Drug Discov.* **2003**, *2*, 140–150.
9. Douglas, D.J.; Frank, A.J.; Mao, D. Linear Ion Traps in Mass Spectrometry. *Mass Spectrom. Rev.* **2005**, *24*, 1–29.
10. Hondo, T.; Kawai, Y.; Toyoda, M. Signal-to-Noise Performance Evaluation of a New 12-Bit Digitizer on a Time-of-Flight Mass Spectrometer. *Eur. J. Mass Spectrom.* **2015**, *21*, 13–17.
11. Makarov, A.; Denisov, E.; Lange, O.; Horning, S. Dynamic Range of Mass Accuracy in LTQ Orbitrap Hybrid Mass Spectrometer. *J. Am. Soc. Mass Spectrom.* **2006**, *17*, 977–982.
12. Eliuk, S.; Makarov, A. Evolution of Orbitrap Mass Spectrometry Instrumentation. *Annu. Rev. Anal. Chem.* **2015**, *8*, 61–80.
13. Bowman, A.P.; Blakney, G.T.; Hendrickson, C.L.; Ellis, S.R.; Heeren, R.M.A.; Smith, D.F. Ultra-High Mass Resolving Power, Mass Accuracy, and Dynamic Range MALDI Mass Spectrometry Imaging by 21-T FT-ICR MS. *Anal. Chem.* **2020**, *92*, 3133–3142.
14. Bahureksa, W.; Borch, T.; Young, R.B.; Weisbrod, C.R.; Blakney, G.T.; McKenna, A.M. Improved Dynamic Range, Resolving Power, and Sensitivity Achievable with FT-ICR Mass Spectrometry at 21 T Reveals the Hidden Complexity of Natural Organic Matter. *Anal. Chem.* **2022**, *94*, 11382–11389.
15. Shaw, J.B.; Lin, T.-Y.; Leach, F.E.I.I.I.; Tolmachev, A. V; Tolić, N.; Robinson, E.W.; Koppenaal, D.W.; Paša-Tolić, L. 21 Tesla Fourier Transform Ion Cyclotron Resonance Mass Spectrometer Greatly Expands Mass Spectrometry Toolbox. *J. Am. Soc. Mass Spectrom.* **2016**, *27*, 1929–1936.

16. Jedrychowski, M.P.; Huttlin, E.L.; Haas, W.; Sowa, M.E.; Rad, R.; Gygi, S.P. Evaluation of HCD- and CID-Type Fragmentation Within Their Respective Detection Platforms For Murine Phosphoproteomics*. *Mol. Cell. Proteomics* **2011**, *10*, M111.009910.
17. Francischini, D.S.; Arruda, M.A.Z. When a Picture Is Worth a Thousand Words: Molecular and Elemental Imaging Applied to Environmental Analysis – A Review. *Microchem. J.* **2021**, *169*, 106526.
18. Sussulini, A.; Becker, J.S.; Becker, J.S. Laser Ablation ICP-MS: Application in Biomedical Research. *Mass Spectrom. Rev.* **2017**, *36*, 47–57.
19. Jolivet, L.; Leprince, M.; Moncayo, S.; Sorbier, L.; Lienemann, C.-P.; Motto-Ros, V. Review of the Recent Advances and Applications of LIBS-Based Imaging. *Spectrochim. Acta Part B At. Spectrosc.* **2019**, *151*, 41–53.
20. Zhang, R.; Li, L.; Sultanbawa, Y.; Xu, Z.P. X-Ray Fluorescence Imaging of Metals and Metalloids in Biological Systems. *Am. J. Nucl. Med. Mol. Imaging* **2018**, *8*, 169–188.
21. Baker, T.C.; Han, J.; Borchers, C.H. Recent Advancements in Matrix-Assisted Laser Desorption/Ionization Mass Spectrometry Imaging. *Curr. Opin. Biotechnol.* **2017**, *43*, 62–69.
22. Xue, J.; Bai, Y.; Liu, H. Recent Advances in Ambient Mass Spectrometry Imaging. *TrAC - Trends Anal. Chem.* **2019**, *120*, 115659.
23. Chung, H.-H.; Huang, P.; Chen, C.-L.; Lee, C.; Hsu, C.-C. Next-Generation Pathology Practices with Mass Spectrometry Imaging. *Mass Spectrom. Rev.* **2022**, e21795.
24. Wang, T.; Cheng, X.; Xu, H.; Meng, Y.; Yin, Z.; Li, X.; Hang, W. Perspective on Advances in Laser-Based High-Resolution Mass Spectrometry Imaging. *Anal. Chem.* **2020**, *92*, 543–553.
25. Gilmore, I.S.; Heiles, S.; Pieterse, C.L. Metabolic Imaging at the Single-Cell Scale: Recent Advances in Mass Spectrometry Imaging. *Annu. Rev. Anal. Chem.* **2019**, *12*, 201–226.
26. Porta Siegel, T.; Hamm, G.; Bunch, J.; Cappell, J.; Fletcher, J.S.; Schwamborn, K. Mass Spectrometry Imaging and Integration with Other Imaging Modalities for Greater Molecular Understanding of Biological Tissues. *Mol. Imaging Biol.* **2018**, *20*, 888–901.
27. Cole, L.M.; Handley, J.; Claude, E.; Duckett, C.J.; Mudhar, H.S.; Sisley, K.; Clench, M.R. Multi-Modal Mass Spectrometric Imaging of Uveal Melanoma. *Metabolites* 2021, *11*.
28. Hagvall, L.; Pour, M.D.; Feng, J.; Karma, M.; Hedberg, Y.; Malmberg, P. Skin Permeation of Nickel, Cobalt and Chromium Salts in Ex Vivo Human Skin, Visualized Using Mass Spectrometry Imaging. *Toxicol. Vitr.* **2021**, *76*, 105232.
29. Kaya, I.; Jennische, E.; Lange, S.; Malmberg, P. Multimodal Chemical Imaging of a Single Brain Tissue Section Using ToF-SIMS, MALDI-ToF and Immuno/Histochemical Staining. *Analyst* **2021**, *146*, 1169–1177.
30. Philipsen, M.H.; Haxen, E.R.; Manaprasertsak, A.; Malmberg, P.; Hammarlund, E.U. Mapping the Chemistry of Hair Strands by Mass Spectrometry Imaging - A Review. *Molecules* 2021, *26*.
31. Fletcher, J.S. Cellular Imaging with Secondary Ion Mass Spectrometry. *Analyst* **2009**, *134*, 2204–2215.
32. Li, K.; Liu, J.; Grovenor, C.R.M.; Moore, K.L. NanoSIMS Imaging and Analysis in Materials Science. *Annu. Rev. Anal. Chem.* **2020**, *13*, 273–292.

33. Maharrey, S.; Bastasz, R.; Behrens, R.; Highley, A.; Hoffer, S.; Kruppa, G.; Whaley, J. High Mass Resolution SIMS. *Appl. Surf. Sci.* **2004**, *231–232*, 972–975.
34. Passarelli, M.K.; Pirkl, A.; Moellers, R.; Grinfeld, D.; Kollmer, F.; Havelund, R.; Newman, C.F.; Marshall, P.S.; Arlinghaus, H.; Alexander, M.R.; et al. The 3D OrbiSIMS—Label-Free Metabolic Imaging with Subcellular Lateral Resolution and High Mass-Resolving Power. *Nat. Methods* **2017**, *14*, 1175–1183.
35. Spengler, B.; Hubert, M.; Kaufmann, R. MALDI Ion Imaging and Biological Ion Imaging with a New Scanning UV-Laser Microprobe. In Proceedings of the 42nd ASMS Conference on Mass Spectrometry and Allied Topics; 1994; p. 1041.
36. Caprioli, R.M.; Farmer, T.B.; Gile, J. Molecular Imaging of Biological Samples: Localization of Peptides and Proteins Using MALDI-TOF MS. *Anal. Chem.* **1997**, *69*, 4751–4760.
37. Chang, W.C.; Huang, L.C.L.; Wang, Y.-S.; Peng, W.-P.; Chang, H.C.; Hsu, N.Y.; Yang, W. Bin; Chen, C.H. Matrix-Assisted Laser Desorption/Ionization (MALDI) Mechanism Revisited. *Anal. Chim. Acta* **2007**, *582*, 1–9.
38. Zenobi, R.; Knochenmuss, R. Ion Formation in MALDI Mass Spectrometry. *Mass Spectrom. Rev.* **1998**, *17*, 337–366.
39. Karas, M.; Krüger, R. Ion Formation in MALDI: The Cluster Ionization Mechanism. *Chem. Rev.* **2003**, *103*, 427–440.
40. Zhou, Q.; Fülöp, A.; Hopf, C. Recent Developments of Novel Matrices and On-Tissue Chemical Derivatization Reagents for MALDI-MSI. *Anal. Bioanal. Chem.* **2021**, *413*, 2599–2617.
41. Kompauer, M.; Heiles, S.; Spengler, B. Atmospheric Pressure MALDI Mass Spectrometry Imaging of Tissues and Cells at 1.4-μm Lateral Resolution. *Nat. Methods* **2017**, *14*, 90–96.
42. Soltwisch, J.; Kettling, H.; Vens-Cappell, S.; Wiegelmann, M.; Müthing, J.; Dreisewerd, K. Mass Spectrometry Imaging with Laser-Induced Postionization. *Science (80-.).* **2015**, *348*, 211–215.
43. Niehaus, M.; Soltwisch, J.; Belov, M.E.; Dreisewerd, K. Transmission-Mode MALDI-2 Mass Spectrometry Imaging of Cells and Tissues at Subcellular Resolution. *Nat. Methods* **2019**, *16*, 925–931.
44. Trim, P.J.; Snel, M.F. Small Molecule MALDI MS Imaging: Current Technologies and Future Challenges. *Methods* **2016**, *104*, 127–141.
45. Cech, N.B.; Enke, C.G. Practical Implications of Some Recent Studies in Electrospray Ionization Fundamentals. *Mass Spectrom. Rev.* **2001**, *20*, 362–387.
46. Wilm, M. Principles of Electrospray Ionization. *Mol. Cell. Proteomics* **2011**, *10*, M111.009407.
47. Iribarne, J. V; Thomson, B.A. On the Evaporation of Small Ions from Charged Droplets. *J. Chem. Phys.* **2008**, *64*, 2287–2294.
48. Thomson, B.A.; Iribarne, J. V Field Induced Ion Evaporation from Liquid Surfaces at Atmospheric Pressure. *J. Chem. Phys.* **2008**, *71*, 4451–4463.
49. Wilm, M.S.; Mann, M. Electrospray and Taylor-Cone Theory, Dole's Beam of Macromolecules at Last? *Int. J. Mass Spectrom. Ion Process.* **1994**, *136*, 167–180.
50. Dole, M.; Mack, L.L.; Hines, R.L.; Mobley, R.C.; Ferguson, L.D.; Alice, M.B. Molecular Beams of Macroions. *J. Chem. Phys.* **2003**, *49*, 2240–2249.
51. Konermann, L.; Ahadi, E.; Rodriguez, A.D.; Vahidi, S. Unraveling the Mechanism of Electrospray Ionization. *Anal. Chem.* **2013**, *85*, 2–9.

52. Taylor, G.I. Disintegration of Water Drops in an Electric Field. *Proc. R. Soc. London. Ser. A. Math. Phys. Sci.* **1997**, *280*, 383–397.
53. Fenn, J.B.; Mann, M.; Meng, C.K.A.I.; Wong, S.F.; Whitehouse, C.M. Electrospray Ionization for Mass Spectrometry of Large Biomolecules. *Science (80-.).* **1989**, *246*, 64–71.
54. Tanaka, K.; Waki, H.; Ido, Y.; Akita, S.; Yoshida, Y.; Yoshida, T.; Matsuo, T. Protein and Polymer Analyses up to m/z 100 000 by Laser Ionization Time-of-Flight Mass Spectrometry. *Rapid Commun. Mass Spectrom.* **1988**, *2*, 151–153.
55. Gaskell, S.J. Electrospray: Principles and Practice. *J. Mass Spectrom.* **1997**, *32*, 677–688.
56. Juraschek, R.; Dülcks, T.; Karas, M. Nanoelectrospray—More than Just a Minimized-Flow Electrospray Ionization Source. *J. Am. Soc. Mass Spectrom.* **1999**, *10*, 300–308.
57. El-Faramawy, A.; Siu, K.W.M.; Thomson, B.A. Efficiency of Nano-Electrospray Ionization. *J. Am. Soc. Mass Spectrom.* **2005**, *16*, 1702–1707.
58. Cech, N.B.; Enke, C.G. Effect of Affinity for Droplet Surfaces on the Fraction of Analyte Molecules Charged during Electrospray Droplet Fission. *Anal. Chem.* **2001**, *73*, 4632–4639.
59. Takáts, Z.; Wiseman, J.M.; Gologan, B.; Cooks, R.G. Mass Spectrometry Sampling Under Ambient Conditions with Desorption Electrospray Ionization. *Science (80-.).* **2004**, *306*, 471–473.
60. Ifa, D.R.; Wiseman, J.M.; Song, Q.; Cooks, R.G. Development of Capabilities for Imaging Mass Spectrometry under Ambient Conditions with Desorption Electrospray Ionization (DESI). *Int. J. Mass Spectrom.* **2007**, *259*, 8–15.
61. He, M.J.; Pu, W.; Wang, X.; Zhang, W.; Tang, D.; Dai, Y. Comparing DESI-MSI and MALDI-MSI Mediated Spatial Metabolomics and Their Applications in Cancer Studies . *Front. Oncol.* 2022, *12*.
62. Swales, J.G.; Hamm, G.; Clench, M.R.; Goodwin, R.J.A. Mass Spectrometry Imaging and Its Application in Pharmaceutical Research and Development: A Concise Review. *Int. J. Mass Spectrom.* **2019**, *437*, 99–112.
63. Wu, C.; Dill, A.L.; Eberlin, L.S.; Cooks, R.G.; Ifa, D.R. Mass Spectrometry Imaging under Ambient Conditions. *Mass Spectrom. Rev.* **2013**, *32*, 218–243.
64. Roach, P.J.; Laskin, J.; Laskin, A. Nanospray Desorption Electrospray Ionization: An Ambient Method for Liquid-Extraction Surface Sampling in Mass Spectrometry. *Analyst* **2010**, *135*, 2233–2236.
65. Laskin, J.; Heath, B.S.; Roach, P.J.; Cazares, L.; Semmes, O.J. Tissue Imaging Using Nanospray Desorption Electrospray Ionization Mass Spectrometry. *Anal. Chem.* **2012**, *84*, 141–148.
66. Lanekoff, I.; Laskin, J. Imaging of Lipids and Metabolites Using Nanospray Desorption Electrospray Ionization Mass Spectrometry BT - Mass Spectrometry Imaging of Small Molecules. In; He, L., Ed.; Springer New York: New York, NY, 2015; pp. 99–106 ISBN 978-1-4939-1357-2.
67. Li, N.; Nie, H.; Jiang, L.; Ruan, G.; Du, F.; Liu, H. Recent Advances of Ambient Ionization Mass Spectrometry Imaging in Clinical Research. *J. Sep. Sci.* **2020**, *43*, 3146–3163.
68. Xiao, Y.; Deng, J.; Yao, Y.; Fang, L.; Yang, Y.; Luan, T. Recent Advances of Ambient Mass Spectrometry Imaging for Biological Tissues: A Review. *Anal. Chim. Acta* **2020**, *1117*, 74–88.
69. Duncan, K.D.; Bergman, H.M.; Lanekoff, I. A Pneumatically Assisted Nanospray Desorption Electrospray Ionization Source for Increased Solvent Versatility and Enhanced Metabolite Detection from Tissue. *Analyst* **2017**, *142*, 3424–3431.

70. Santos, V.G.; Regiani, T.; Dias, F.F.G.; Romao, W.; Jara, J.L.P.; Klitzke, C.F.; Coelho, F.; Eberlin, M.N. Venturi Easy Ambient Sonic-Spray Ionization. *Anal. Chem.* **2011**, *83*, 1375–1380.
71. Mavroudakis, L.; Lanekoff, I. Ischemic Stroke Causes Disruptions in the Carnitine Shuttle System. *Metabolites* **2023**, *13*, 278.
72. Mavroudakis, L.; Duncan, K.D.; Lanekoff, I. Host-Guest Chemistry for Simultaneous Imaging of Endogenous Alkali Metals and Metabolites with Mass Spectrometry. *Anal. Chem.* **2022**, *94*, 2391–2398.
73. Lillja, J.; Duncan, K.D.; Lanekoff, I. Determination of Monounsaturated Fatty Acid Isomers in Biological Systems by Modeling MS3 Product Ion Patterns. *J. Am. Soc. Mass Spectrom.* **2020**, *31*, 2479–2487.
74. Mavroudakis, L.; Lanekoff, I. Matrix Effects Free Imaging of Thin Tissue Sections Using Pneumatically Assisted Nano-DESI MSI BT - Imaging Mass Spectrometry: Methods and Protocols. In; Cole, L.M., Clench, M.R., Eds.; Springer US: New York, NY, 2023; pp. 107–121 ISBN 978-1-0716-3319-9.
75. Weigand, M.R.; Yang, M.; Hu, H.; Zensho, C.; Laskin, J. Enhancement of Lipid Signals with Ammonium Fluoride in Negative Mode Nano-DESI Mass Spectrometry Imaging. *Int. J. Mass Spectrom.* **2022**, *478*, 116859.
76. Unsihuay, D.; Qiu, J.; Swaroop, S.; Nagornov, K.O.; Kozhinov, A.N.; Tsybin, Y.O.; Kuang, S.; Laskin, J. Imaging of Triglycerides in Tissues Using Nanospray Desorption Electrospray Ionization (Nano-DESI) Mass Spectrometry. *Int. J. Mass Spectrom.* **2020**, *448*, 116269.
77. Wu, C.; Ifa, D.R.; Manicke, N.E.; Cooks, R.G. Rapid, Direct Analysis of Cholesterol by Charge Labeling in Reactive Desorption Electrospray Ionization. *Anal. Chem.* **2009**, *81*, 7618–7624.
78. Laskin, J.; Eckert, P.A.; Roach, P.J.; Heath, B.S.; Nizkorodov, S.A.; Laskin, A. Chemical Analysis of Complex Organic Mixtures Using Reactive Nanospray Desorption Electrospray Ionization Mass Spectrometry. *Anal. Chem.* **2012**, *84*, 7179–7187.
79. Huang, G.; Chen, H.; Zhang, X.; Cooks, R.G.; Ouyang, Z. Rapid Screening of Anabolic Steroids in Urine by Reactive Desorption Electrospray Ionization. *Anal. Chem.* **2007**, *79*, 8327–8332.
80. Kaya, I.; Schembri, L.S.; Nilsson, A.; Shariatgorji, R.; Baijnath, S.; Zhang, X.; Bezard, E.; Svenningsson, P.; Odell, L.R.; Andrén, P.E. On-Tissue Chemical Derivatization for Comprehensive Mapping of Brain Carboxyl and Aldehyde Metabolites by MALDI–MS Imaging. *J. Am. Soc. Mass Spectrom.* **2023**, *34*, 836–846.
81. Shariatgorji, M.; Nilsson, A.; Fridjonsdottir, E.; Vallianatou, T.; Källback, P.; Katan, L.; Sävmarker, J.; Mantas, I.; Zhang, X.; Bezard, E.; et al. Comprehensive Mapping of Neurotransmitter Networks by MALDI–MS Imaging. *Nat. Methods* **2019**, *16*, 1021–1028.
82. Hale, O.J.; Cooper, H.J. Native Ambient Mass Spectrometry of an Intact Membrane Protein Assembly and Soluble Protein Assemblies Directly from Lens Tissue. *Angew. Chemie Int. Ed.* **2022**, *61*, e202201458.
83. Hale, O.J.; Cooper, H.J. Native Mass Spectrometry Imaging of Proteins and Protein Complexes by Nano-DESI. *Anal. Chem.* **2021**, *93*, 4619–4627.
84. Hale, O.J.; Hughes, J.W.; Sisley, E.K.; Cooper, H.J. Native Ambient Mass Spectrometry Enables Analysis of Intact Endogenous Protein Assemblies up to 145 kDa Directly from Tissue. *Anal. Chem.* **2022**, *94*, 5608–5614.

85. Hale, O.J.; Hughes, J.W.; Cooper, H.J. Simultaneous Spatial, Conformational, and Mass Analysis of Intact Proteins and Protein Assemblies by Nano-DESI Travelling Wave Ion Mobility Mass Spectrometry Imaging. *Int. J. Mass Spectrom.* **2021**, *468*, 116656.
86. Sisley, E.K.; Hale, O.J.; Styles, I.B.; Cooper, H.J. Native Ambient Mass Spectrometry Imaging of Ligand-Bound and Metal-Bound Proteins in Rat Brain. *J. Am. Chem. Soc.* **2022**, *144*, 2120–2128.
87. Illes-Toth, E.; Hale, O.J.; Hughes, J.W.; Strittmatter, N.; Rose, J.; Clayton, B.; Sargeant, R.; Jones, S.; Dannhorn, A.; Goodwin, R.J.A.; et al. Mass Spectrometry Detection and Imaging of a Non-Covalent Protein–Drug Complex in Tissue from Orally Dosed Rats. *Angew. Chemie Int. Ed.* **2022**, *61*, e202202075.
88. Lillja, J.; Lanekoff, I. Quantitative Determination of Sn-Positional Phospholipid Isomers in MSn Using Silver Cationization. *Anal. Bioanal. Chem.* **2022**, *414*, 7473–7482.
89. Jackson, A.U.; Shum, T.; Sokol, E.; Dill, A.; Cooks, R.G. Enhanced Detection of Olefins Using Ambient Ionization Mass Spectrometry: Ag+ Adducts of Biologically Relevant Alkenes. *Anal. Bioanal. Chem.* **2011**, *399*, 367–376.
90. Yoo, H.J.; Håkansson, K. Determination of Phospholipid Regiochemistry by Ag(I) Adduction and Tandem Mass Spectrometry. *Anal. Chem.* **2011**, *83*, 1275–1283.
91. Duncan, K.D.; Fang, R.; Yuan, J.; Chu, R.K.; Dey, S.K.; Burnum-Johnson, K.E.; Lanekoff, I. Quantitative Mass Spectrometry Imaging of Prostaglandins as Silver Ion Adducts with Nanospray Desorption Electrospray Ionization. *Anal. Chem.* **2018**, *90*, 7246–7252.
92. Ieritano, C.; Thomas, P.; Hopkins, W.S. Argentination: A Silver Bullet for Cannabinoid Separation by Differential Mobility Spectrometry. *Anal. Chem.* **2023**, *95*, 8668–8678.
93. Maccarone, A.T.; Duldig, J.; Mitchell, T.W.; Blanksby, S.J.; Duchoslav, E.; Campbell, J.L. Characterization of Acyl Chain Position in Unsaturated Phosphatidylcholines Using Differential Mobility-Mass Spectrometry. *J. Lipid Res.* **2014**, *55*, 1668–1677.
94. Kirschbaum, C.; Greis, K.; Gewinner, S.; Schöllkopf, W.; Meijer, G.; von Helden, G.; Pagel, K. Cryogenic Infrared Spectroscopy Provides Mechanistic Insight into the Fragmentation of Phospholipid Silver Adducts. *Anal. Bioanal. Chem.* **2022**, *414*, 5275–5285.
95. Russo, C.; Lewis, E.E.L.; Flint, L.; Clench, M.R. Mass Spectrometry Imaging of 3D Tissue Models. *Proteomics* **2018**, *18*, 1700462.
96. Römpp, A.; Spengler, B. Mass Spectrometry Imaging with High Resolution in Mass and Space. *Histochem. Cell Biol.* **2013**, *139*, 759–783.
97. Buchberger, A.R.; DeLaney, K.; Johnson, J.; Li, L. Mass Spectrometry Imaging: A Review of Emerging Advancements and Future Insights. *Anal. Chem.* **2018**, *90*, 240–265.
98. Cole, L.M.; Clench, M.R. Mass Spectrometry Imaging Tools in Oncology. *Biomark. Med.* **2015**, *9*, 863–868.
99. Lanekoff, I.; Heath, B.S.; Liyu, A.; Thomas, M.; Carson, J.P.; Laskin, J. Automated Platform for High-Resolution Tissue Imaging Using Nanospray Desorption Electrospray Ionization Mass Spectrometry. *Anal. Chem.* **2012**, *84*, 8351–8356.

100. Robichaud, G.; Garrard, K.P.; Barry, J.A.; Muddiman, D.C. MSiReader: An Open-Source Interface to View and Analyze High Resolving Power MS Imaging Files on Matlab Platform. *J. Am. Soc. Mass Spectrom.* **2013**, *24*, 718–721.
101. Lillja, J.; Duncan, K.; Lanekoff, I. Ion-to-Image, i2i, a New Mass Spectrometry Imaging Data Analysis Platform for Continuous Ionization Techniques. *Anal. Chem.* **2023**, *95*, 11589–11595.
102. Flinders, B.; Morrell, J.; Marshall, P.S.; Ranshaw, L.E.; Heeren, R.M.A.; Clench, M.R. Monitoring the Three-Dimensional Distribution of Endogenous Species in the Lungs by Matrix-Assisted Laser Desorption/Ionization Mass Spectrometry Imaging. *Rapid Commun. Mass Spectrom.* **2021**, *35*, e8957.
103. Lanekoff, I.; Burnum-Johnson, K.; Thomas, M.; Cha, J.; Dey, S.K.; Yang, P.; Prieto Conaway, M.C.; Laskin, J. Three-Dimensional Imaging of Lipids and Metabolites in Tissues by Nanospray Desorption Electrospray Ionization Mass Spectrometry. *Anal. Bioanal. Chem.* **2015**, *407*, 2063–2071.
104. Xiong, X.; Xu, W.; Eberlin, L.S.; Wiseman, J.M.; Fang, X.; Jiang, Y.; Huang, Z.; Zhang, Y.; Cooks, R.G.; Ouyang, Z. Data Processing for 3D Mass Spectrometry Imaging. *J. Am. Soc. Mass Spectrom.* **2012**, *23*, 1147–1156.
105. Rzagalinski, I.; Volmer, D.A. Quantification of Low Molecular Weight Compounds by MALDI Imaging Mass Spectrometry – A Tutorial Review. *Biochim. Biophys. Acta - Proteins Proteomics* **2017**, *1865*, 726–739.
106. Deininger, S.O.; Cornett, D.S.; Paape, R.; Becker, M.; Pineau, C.; Rauser, S.; Walch, A.; Wolski, E. Normalization in MALDI-TOF Imaging Datasets of Proteins: Practical Considerations. *Anal. Bioanal. Chem.* **2011**, *401*, 167–181.
107. Fonville, J.M.; Carter, C.; Cloarec, O.; Nicholson, J.K.; Lindon, J.C.; Bunch, J.; Holmes, E. Robust Data Processing and Normalization Strategy for MALDI Mass Spectrometric Imaging. *Anal. Chem.* **2012**, *84*, 1310–1319.
108. Lanekoff, I.; Stevens, S.L.; Stenzel-Poore, M.P.; Laskin, J. Matrix Effects in Biological Mass Spectrometry Imaging: Identification and Compensation. *Analyst* **2014**, *139*, 3528–3532.
109. Hamm, G.; Bonnel, D.; Legouffe, R.; Pamelard, F.; Delbos, J.-M.; Bouzom, F.; Stauber, J. Quantitative Mass Spectrometry Imaging of Propranolol and Olanzapine Using Tissue Extinction Calculation as Normalization Factor. *J. Proteomics* **2012**, *75*, 4952–4961.
110. Taylor, A.J.; Dexter, A.; Bunch, J. Exploring Ion Suppression in Mass Spectrometry Imaging of a Heterogeneous Tissue. *Anal. Chem.* **2018**, *90*, 5637–5645.
111. Groseclose, M.R.; Castellino, S. A Mimetic Tissue Model for the Quantification of Drug Distributions by MALDI Imaging Mass Spectrometry. *Anal. Chem.* **2013**, *85*, 10099–10106.
112. Barry, J.; Barry, J.A.; Groseclose, M.R.; Fraser, D.D.; Castellino, S. Revised Preparation of a Mimetic Tissue Model for Quantitative Imaging Mass Spectrometry. *Protoc. Exch.* **2018**, 1–20.
113. Hewavitharana, A.K. Matrix Matching in Liquid Chromatography–Mass Spectrometry with Stable Isotope Labelled Internal Standards—Is It Necessary? *J. Chromatogr. A* **2011**, *1218*, 359–361.
114. Tobias, F.; Hummon, A.B. Considerations for MALDI-Based Quantitative Mass Spectrometry Imaging Studies. *J. Proteome Res.* **2020**, *19*, 3620–3630.
115. Unsihuay, D.; Mesa Sanchez, D.; Laskin, J. Quantitative Mass Spectrometry Imaging of Biological Systems. *Annu. Rev. Phys. Chem.* **2021**, *72*, 307–329.

116. Chumbley, C.W.; Reyzer, M.L.; Allen, J.L.; Marriner, G.A.; Via, L.E.; Barry, C.E.I.I.I.; Caprioli, R.M. Absolute Quantitative MALDI Imaging Mass Spectrometry: A Case of Rifampicin in Liver Tissues. *Anal. Chem.* **2016**, *88*, 2392–2398.
117. Källback, P.; Shariatgorji, M.; Nilsson, A.; Andrén, P.E. Novel Mass Spectrometry Imaging Software Assisting Labeled Normalization and Quantitation of Drugs and Neuropeptides Directly in Tissue Sections. *J. Proteomics* **2012**, *75*, 4941–4951.
118. Lanekoff, I.; Thomas, M.; Carson, J.P.; Smith, J.N.; Timchalk, C.; Laskin, J. Imaging Nicotine in Rat Brain Tissue by Use of Nanospray Desorption Electrospray Ionization Mass Spectrometry. *Anal. Chem.* **2013**, *85*, 882–889.
119. Peters, F.T.; Maurer, H.H. Systematic Comparison of Bias and Precision Data Obtained with Multiple-Point and One-Point Calibration in Six Validated Multianalyte Assays for Quantification of Drugs in Human Plasma. *Anal. Chem.* **2007**, *79*, 4967–4976.
120. Fornal, E.; Stachniuk, A. Application of a Truly One-Point Calibration for Pesticide Residue Control by Liquid Chromatography–Mass Spectrometry. *J. Chromatogr. B* **2012**, *901*, 107–114.
121. Dewez, F.; De Pauw, E.; Heeren, R.M.A.; Balluff, B. Multilabel Per-Pixel Quantitation in Mass Spectrometry Imaging. *Anal. Chem.* **2021**, 0–7.
122. Zubair, F.; Prentice, B.M.; Norris, J.L.; Laibinis, P.E.; Caprioli, R.M. Standard Reticle Slide To Objectively Evaluate Spatial Resolution and Instrument Performance in Imaging Mass Spectrometry. *Anal. Chem.* **2016**, *88*, 7302–7311.
123. Yin, R.; Burnum-Johnson, K.E.; Sun, X.; Dey, S.K.; Laskin, J. High Spatial Resolution Imaging of Biological Tissues Using Nanospray Desorption Electrospray Ionization Mass Spectrometry. *Nat. Protoc.* **2019**, *14*, 3445–3470.
124. Nguyen, S.N.; Sontag, R.L.; Carson, J.P.; Corley, R.A.; Ansong, C.; Laskin, J. Towards High-Resolution Tissue Imaging Using Nanospray Desorption Electrospray Ionization Mass Spectrometry Coupled to Shear Force Microscopy. *J. Am. Soc. Mass Spectrom.* **2018**, *29*, 316–322.
125. Metodiev, M.D.; Steven, R.T.; Loizeau, X.; Takats, Z.; Bunch, J. Modality Agnostic Model for Spatial Resolution in Mass Spectrometry Imaging: Application to MALDI MSI Data. *Anal. Chem.* **2021**, *93*, 15295–15305.
126. Colliver, T.L.; Brummel, C.L.; Pacholski, M.L.; Swanek, F.D.; Ewing, A.G.; Winograd, N. Atomic and Molecular Imaging at the Single-Cell Level with TOF-SIMS. *Anal. Chem.* **1997**, *69*, 2225–2231.
127. Luxembourg, S.L.; Mize, T.H.; McDonnell, L.A.; Heeren, R.M.A. High-Spatial Resolution Mass Spectrometric Imaging of Peptide and Protein Distributions on a Surface. *Anal. Chem.* **2004**, *76*, 5339–5344.
128. Jiang, L.-X.; Yang, M.; Wali, S.N.; Laskin, J. High-Throughput Mass Spectrometry Imaging of Biological Systems: Current Approaches and Future Directions. *TrAC Trends Anal. Chem.* **2023**, *163*, 117055.
129. Goodwin, R.J.A. Sample Preparation for Mass Spectrometry Imaging: Small Mistakes Can Lead to Big Consequences. *J. Proteomics* **2012**, *75*, 4893–4911.
130. Charles W. Scouten, undefined; Miles Cunningham, undefined Freezing Biological Samples. *Micros. Today* **2006**, *14*, 48.
131. Sugiura, Y.; Shimma, S.; Setou, M. Thin Sectioning Improves the Peak Intensity and Signal-to-Noise Ratio in Direct Tissue Mass Spectrometry. *J. Mass Spectrom. Soc. Jpn.* **2006**, *54*, 45–48.

132. Schwartz, S.A.; Reyzer, M.L.; Caprioli, R.M. Direct Tissue Analysis Using Matrix-Assisted Laser Desorption/Ionization Mass Spectrometry: Practical Aspects of Sample Preparation. *J. Mass Spectrom.* **2003**, *38*, 699–708.
133. Chaurand, P.; L. Norris, J.; Shannon Cornett, D.; A. Mobley, J.; M. Caprioli, R. New Developments in Profiling and Imaging of Proteins from Tissue Sections by MALDI Mass Spectrometry. *J. Proteome Res.* **2006**, *5*, 2889–2900.
134. Grossman, P.D.; Colburn, J.C. *Capillary Electrophoresis: Theory and Practice*; Academic Press: San Diego, CA, 2012; ISBN 9780323138192.
135. Swinney, K.; Bornhop, D.J. Detection in Capillary Electrophoresis. *Electrophoresis* **2000**, *21*, 1239–1250.
136. García, A.; Godzien, J.; López-Gonzálvez, Á.; Barbas, C. Capillary Electrophoresis Mass Spectrometry as a Tool for Untargeted Metabolomics. *Bioanalysis* **2016**, *9*, 99–130.
137. Hirayama, A.; Abe, H.; Yamaguchi, N.; Tabata, S.; Tomita, M.; Soga, T. Development of a Sheathless CE-ESI-MS Interface. *Electrophoresis* **2018**, *39*, 1382–1389.
138. Zhang, W.; Ramautar, R. CE-MS for Metabolomics: Developments and Applications in the Period 2018–2020. *Electrophoresis* **2021**, *42*, 381–401.
139. Dilillo, M.; Pellegrini, D.; Ait-Belkacem, R.; de Graaf, E.L.; Caleo, M.; McDonnell, L.A. Mass Spectrometry Imaging, Laser Capture Microdissection, and LC-MS/MS of the Same Tissue Section. *J. Proteome Res.* **2017**, *16*, 2993–3001.
140. Van Berkel, G.J.; Kertesz, V. Continuous-Flow Liquid Microjunction Surface Sampling Probe Connected on-Line with High-Performance Liquid Chromatography/Mass Spectrometry for Spatially Resolved Analysis of Small Molecules and Proteins. *Rapid Commun. Mass Spectrom.* **2013**, *27*, 1329–1334.
141. Kertesz, V.; Van Berkel, G.J. Liquid Microjunction Surface Sampling Coupled with High-Pressure Liquid Chromatography−Electrospray Ionization-Mass Spectrometry for Analysis of Drugs and Metabolites in Whole-Body Thin Tissue Sections. *Anal. Chem.* **2010**, *82*, 5917–5921.
142. Duncan, K.D.; Lanekoff, I. Spatially Defined Surface Sampling Capillary Electrophoresis Mass Spectrometry. *Anal. Chem.* **2019**, *91*, 7819–7827.
143. Golubova, A.; Lanekoff, I. Surface Sampling Capillary Electrophoresis–Mass Spectrometry for a Direct Chemical Characterization of Tissue and Blood Samples. *Electrophoresis* **2023**, *44*, 387–394.
144. Pan, C.; Wang, W.; Chen, X. In Situ Rapid Preparation of Homochiral Metal-Organic Framework Coated Column for Open Tubular Capillary Electrochromatography. *J. Chromatogr. A* **2016**, *1427*, 125–133.
145. Rodrigues, K.T.; Mekahli, D.; Tavares, M.F.M.; Van Schepdael, A. Development and Validation of a CE-MS Method for the Targeted Assessment of Amino Acids in Urine. *Electrophoresis* **2016**, *37*, 1039–1047.
146. Mantovani, V.; Galeotti, F.; Maccari, F.; Volpi, N. Recent Advances in Capillary Electrophoresis Separation of Monosaccharides, Oligosaccharides, and Polysaccharides. *Electrophoresis* **2018**, *39*, 179–189.
147. Virani, S.S.; Alonso, A.; Benjamin, E.J.; Bittencourt, M.S.; Callaway, C.W.; Carson, A.P.; Chamberlain, A.M.; Chang, A.R.; Cheng, S.; Delling, F.N.; et al. Heart Disease and Stroke Statistics—2020 Update: A Report From the American Heart Association. *Circulation* **2020**, *141*, e139–e596.
148. Catanese, L.; Tarsia, J.; Fisher, M. Acute Ischemic Stroke Therapy Overview. *Circ. Res.* **2017**, *120*, 541–558.

149. Doyle, K.P.; Simon, R.P.; Stenzel-Poore, M.P. Mechanisms of Ischemic Brain Damage. *Neuropharmacology* **2008**, *55*, 310–318.
150. Feske, S.K. Ischemic Stroke. *Am. J. Med.* **2021**, *134*, 1457–1464.
151. Khoshnam, S.E.; Winlow, W.; Farzaneh, M.; Farbood, Y.; Moghaddam, H.F. Pathogenic Mechanisms Following Ischemic Stroke. *Neurol. Sci.* **2017**, *38*, 1167–1186.
152. Yan, Y.; Shapiro, J.I. The Physiological and Clinical Importance of Sodium Potassium ATPase in Cardiovascular Diseases. *Curr. Opin. Pharmacol.* **2016**, *27*, 43–49.
153. Clausen, M.J.V.; Poulsen, H. Sodium/Potassium Homeostasis in the Cell BT - Metallomics and the Cell. In; Banci, L., Ed.; Springer Netherlands: Dordrecht, 2013; pp. 41–67 ISBN 978-94-007-5561-1.
154. Gotoh, O.; Asano, T.; Koide, T.; Takakura, K. Ischemic Brain Edema Following Occlusion of the Middle Cerebral Artery in the Rat. I: The Time Courses of the Brain Water, Sodium and Potassium Contents and Blood-Brain Barrier Permeability to 125I-Albumin. *Stroke* **1985**, *16*, 101–109.
155. Ito, U.; Ohno, K.; Nakamura, R.; Suganuma, F.; Inaba, Y. Brain Edema during Ischemia and after Restoration of Blood Flow. Measurement of Water, Sodium, Potassium Content and Plasma Protein Permeability. *Stroke* **1979**, *10*, 542–547.
156. Ludhiadch, A.; Sharma, R.; Muriki, A.; Munshi, A. Role of Calcium Homeostasis in Ischemic Stroke: A Review. *CNS Neurol. Disord. - Drug Targets* 2022, *21*, 52–61.
157. Liu, F.; Lu, J.; Manaenko, A.; Tang, J.; Hu, Q. Mitochondria in Ischemic Stroke: New Insight and Implications. *Aging Dis.* **2018**, *9*, 924–937.
158. Rabinstein, A.A. Update on Treatment of Acute Ischemic Stroke. *Continuum (Minneap. Minn).* **2020**, *26*, 268–286.
159. Patel, R.A.G.; McMullen, P.W. Neuroprotection in the Treatment of Acute Ischemic Stroke. *Prog. Cardiovasc. Dis.* **2017**, *59*, 542–548.
160. Liang, J.; Han, R.; Zhou, B. Metabolic Reprogramming: Strategy for Ischemic Stroke Treatment by Ischemic Preconditioning. *Biology (Basel).* 2021, *10*.
161. Sommer, C.J. Ischemic Stroke: Experimental Models and Reality. *Acta Neuropathol.* **2017**, *133*, 245–261.
162. Popp, A.; Jaenisch, N.; Witte, O.W.; Frahm, C. Identification of Ischemic Regions in a Rat Model of Stroke. *PLOS ONE* **2009**, *4*, e4764.
163. Cowled, P.; Fitridge, R. Pathophysiology of Reperfusion Injury. In; Fitridge, R., Thompson, M., Eds.; Adelaide (AU), 2011 ISBN 978-0-9871718-2-5.
164. Li, L.; Yang, S.H.; Lemr, K.; Havlicek, V.; Schug, K.A. Continuous Flow-Extractive Desorption Electrospray Ionization: Analysis from "Non-Electrospray Ionization-Friendly" Solvents and Related Mechanism. *Anal. Chim. Acta* **2013**, *769*, 84–90.
165. Lillja, J.; Lanekoff, I. Silver-Doped Nanospray Desorption Electrospray Ionization (Nano-DESI) MSI for Increased Specificity and Sensitivity of Alkenes BT - Mass Spectrometry Imaging of Small Molecules: Methods and Protocols. In; Lee, Y.-J., Ed.; Springer US: New York, NY, 2022; pp. 241–249 ISBN 978-1-0716-2030-4.
166. Duncan, K.D.; Sun, X.; Baker, E.S.; Dey, S.K.; Lanekoff, I. In Situ Imaging Reveals Disparity between Prostaglandin Localization and Abundance of Prostaglandin Synthases. *Commun. Biol.* **2021**, *4*, 1–9.

167. Lin, M.; Blevins, M.S.; Sans, M.; Brodbelt, J.S.; Eberlin, L.S. Deeper Understanding of Solvent-Based Ambient Ionization Mass Spectrometry: Are Molecular Profiles Primarily Dictated by Extraction Mechanisms? *Anal. Chem.* **2022**, *94*, 14734–14744.
168. Kruve, A.; Kaupmees, K.; Liigand, J.; Oss, M.; Leito, I. Sodium Adduct Formation Efficiency in ESI Source. *J. Mass Spectrom.* **2013**, *48*, 695–702.
169. Kruve, A.; Kaupmees, K. Adduct Formation in ESI/MS by Mobile Phase Additives. *J. Am. Soc. Mass Spectrom.* **2017**, *28*, 887–894.
170. Pinho, S.P.; Macedo, E.A. Solubility of NaCl, NaBr, and KCl in Water, Methanol, Ethanol, and Their Mixed Solvents. *J. Chem. Eng. Data* **2005**, *50*, 29–32.
171. Zahn, D.; Meusinger, R.; Frömel, T.; Knepper, T.P. Halomethanesulfonic Acids—A New Class of Polar Disinfection Byproducts: Standard Synthesis, Occurrence, and Indirect Assessment of Mitigation Options. *Environ. Sci. Technol.* **2019**, *53*, 8994–9002.
172. Boulard, L.; Dierkes, G.; Ternes, T. Utilization of Large Volume Zwitterionic Hydrophilic Interaction Liquid Chromatography for the Analysis of Polar Pharmaceuticals in Aqueous Environmental Samples: Benefits and Limitations. *J. Chromatogr. A* **2018**, *1535*, 27–43.
173. Kebarle, P.; Peschke, M. On the Mechanisms by Which the Charged Droplets Produced by Electrospray Lead to Gas Phase Ions. *Anal. Chim. Acta* **2000**, *406*, 11–35.
174. Zhou, S.; Cook, K.D. A Mechanistic Study of Electrospray Mass Spectrometry: Charge Gradients within Electrospray Droplets and Their Influence on Ion Response. *J. Am. Soc. Mass Spectrom.* **2001**, *12*, 206–214.
175. Karas, M.; Bahr, U.; Dülcks, T. Nano-Electrospray Ionization Mass Spectrometry: Addressing Analytical Problems beyond Routine. *Fresenius. J. Anal. Chem.* **2000**, *366*, 669–676.
176. Van De Steene, J.C.; Lambert, W.E. Comparison of Matrix Effects in HPLC-MS/MS and UPLC-MS/MS Analysis of Nine Basic Pharmaceuticals in Surface Waters. *J. Am. Soc. Mass Spectrom.* **2008**, *19*, 713–718.
177. Stüber, M.; Reemtsma, T. Evaluation of Three Calibration Methods to Compensate Matrix Effects in Environmental Analysis with LC-ESI-MS. *Anal. Bioanal. Chem.* **2004**, *378*, 910–916.
178. Lanekoff, I.; Laskin, J. Quantitative Mass Spectrometry Imaging of Molecules in Biological Systems. In *Advances in Chromatography*; Advances in chromatography; CRC Press: Taylor & Francis Group, 6000 Broken Sound Parkway NW, Suite 300, Boca Raton, FL 33487-2742, 2017; pp. 43–72 ISBN 9781315116372.
179. Bergman, H.-M.; Lundin, E.; Andersson, M.; Lanekoff, I. Quantitative Mass Spectrometry Imaging of Small-Molecule Neurotransmitters in Rat Brain Tissue Sections Using Nanospray Desorption Electrospray Ionization. *Analyst* **2016**, *141*, 3686–3695.
180. Lanekoff, I.; Thomas, M.; Laskin, J. Shotgun Approach for Quantitative Imaging of Phospholipids Using Nanospray Desorption Electrospray Ionization Mass Spectrometry. *Anal. Chem.* **2014**, *86*, 1872–1880.
181. Liigand, P.; Liigand, J.; Kaupmees, K.; Kruve, A. 30 Years of Research on ESI/MS Response: Trends, Contradictions and Applications. *Anal. Chim. Acta* **2021**, *1152*, 238117.
182. Liigand, J.; Wang, T.; Kellogg, J.; Smedsgaard, J.; Cech, N.; Kruve, A. Quantification for Non-Targeted LC/MS Screening without Standard Substances. *Sci. Rep.* **2020**, *10*, 5808.

183. Kruve, A. Strategies for Drawing Quantitative Conclusions from Nontargeted Liquid Chromatography–High-Resolution Mass Spectrometry Analysis. *Anal. Chem.* **2020**, *92*, 4691–4699.
184. Bieber, S.; Letzel, T.; Kruve, A. Electrospray Ionization Efficiency Predictions and Analytical Standard Free Quantification for SFC/ESI/HRMS. *J. Am. Soc. Mass Spectrom.* **2023**, *34*, 1511–1518.
185. Inose, Y.; Kato, Y.; Kitagawa, K.; Uchiyama, S.; Shibata, N. Activated Microglia in Ischemic Stroke Penumbra Upregulate MCP-1 and CCR2 Expression in Response to Lysophosphatidylcholine Derived from Adjacent Neurons and Astrocytes. *Neuropathology* **2015**, *35*, 209–223.
186. Wang, H.Y.J.; Liu, C. Bin; Wu, H.W.; Kuo, S. Direct Profiling of Phospholipids and Lysophospholipids in Rat Brain Sections after Ischemic Stroke. *Rapid Commun. Mass Spectrom.* **2010**, *24*, 2057–2064.
187. Zheng, L.; Xie, C.; Zheng, J.; Dong, Q.; Si, T.; Zhang, J.; Hou, S.-T. An Imbalanced Ratio between PC(16:0/16:0) and LPC(16:0) Revealed by Lipidomics Supports the Role of the Lands Cycle in Ischemic Brain Injury. *J. Biol. Chem.* **2021**, *296*, 100151.
188. Schulz, S.; Gerhardt, D.; Meyer, B.; Seegel, M.; Schubach, B.; Hopf, C.; Matheis, K. DMSO-Enhanced MALDI MS Imaging with Normalization against a Deuterated Standard for Relative Quantification of Dasatinib in Serial Mouse Pharmacology Studies. *Anal. Bioanal. Chem.* **2013**, *405*, 9467–9476.
189. Lagarrigue, M.; Lavigne, R.; Tabet, E.; Genet, V.; Thomé, J.-P.; Rondel, K.; Guével, B.; Multigner, L.; Samson, M.; Pineau, C. Localization and in Situ Absolute Quantification of Chlordecone in the Mouse Liver by MALDI Imaging. *Anal. Chem.* **2014**, *86*, 5775–5783.
190. Boudon, S.M.; Morandi, G.; Prideaux, B.; Staab, D.; Junker, U.; Odermatt, A.; Stoeckli, M.; Bauer, D. Evaluation of Sparfloxacin Distribution by Mass Spectrometry Imaging in a Phototoxicity Model. *J. Am. Soc. Mass Spectrom.* **2014**, *25*, 1803–1809.
191. Nakanishi, T.; Takai, S.; Jin, D.; Takubo, T. Quantification of Candesartan in Mouse Plasma by MALDI-TOFMS and in Tissue Sections by MALDI-Imaging Using the Stable-Isotope Dilution Technique. *Mass Spectrom.* **2013**, *2*, A0021.
192. Prideaux, B.; Dartois, V.; Staab, D.; Weiner, D.M.; Goh, A.; Via, L.E.; Barry, C.E.I.I.I.; Stoeckli, M. High-Sensitivity MALDI-MRM-MS Imaging of Moxifloxacin Distribution in Tuberculosis-Infected Rabbit Lungs and Granulomatous Lesions. *Anal. Chem.* **2011**, *83*, 2112–2118.
193. Quiason, C.M.; Shahidi-Latham, S.K. Imaging MALDI MS of Dosed Brain Tissues Utilizing an Alternative Analyte Pre-Extraction Approach. *J. Am. Soc. Mass Spectrom.* **2015**, *26*, 967–973.
194. Ebert, D.; Haller, R.G.; Walton, M.E. Energy Contribution of Octanoate to Intact Rat Brain Metabolism Measured by 13C Nuclear Magnetic Resonance Spectroscopy. *J. Neurosci.* **2003**, *23*, 5928 LP – 5935.
195. Chumachenko, M.S.; Waseem, T. V; Fedorovich, S. V Metabolomics and Metabolites in Ischemic Stroke. *Rev. Neurosci.* **2022**, *33*, 181–205.
196. Wang, X.; Zhang, L.; Sun, W.; Pei, L.L.; Tian, M.; Liang, J.; Liu, X.; Zhang, R.; Fang, H.; Wu, J.; et al. Changes of Metabolites in Acute Ischemic Stroke and Its Subtypes. *Front. Neurosci.* **2021**, *14*, 1–8.

197. Xiang, L.; Wei, J.; Tian, X.Y.; Wang, B.; Chan, W.; Li, S.; Tang, Z.; Zhang, H.; Cheang, W.S.; Zhao, Q.; et al. Comprehensive Analysis of Acylcarnitine Species in Db/Db Mouse Using a Novel Method of High-Resolution Parallel Reaction Monitoring Reveals Widespread Metabolic Dysfunction Induced by Diabetes. *Anal. Chem.* **2017**, *89*, 10368–10375.
198. Oss, M.; Kruve, A.; Herodes, K.; Leito, I. Electrospray Ionization Efficiency Scale of Organic Compounds. *Anal. Chem.* **2010**, *82*, 2865–2872.
199. Kiontke, A.; Oliveira-Birkmeier, A.; Opitz, A.; Birkemeyer, C. Electrospray Ionization Efficiency Is Dependent on Different Molecular Descriptors with Respect to Solvent PH and Instrumental Configuration. *PLOS ONE* **2016**, *11*, e0167502.
200. Chalcraft, K.R.; Lee, R.; Mills, C.; Britz-McKibbin, P. Virtual Quantification of Metabolites by Capillary Electrophoresis-Electrospray Ionization-Mass Spectrometry: Predicting Ionization Efficiency Without Chemical Standards. *Anal. Chem.* **2009**, *81*, 2506–2515.
201. Tang, L.; Kebarle, P. Dependence of Ion Intensity in Electrospray Mass Spectrometry on the Concentration of the Analytes in the Electrosprayed Solution. *Anal. Chem.* **1993**, *65*, 3654–3668.
202. Zuniga, A.; Li, L. Ultra-High Performance Liquid Chromatography Tandem Mass Spectrometry for Comprehensive Analysis of Urinary Acylcarnitines. *Anal. Chim. Acta* **2011**, *689*, 77–84.
203. McClellan, J.E.; Quarmby, S.T.; Yost, R.A. Parent and Neutral Loss Monitoring on a Quadrupole Ion Trap Mass Spectrometer: Screening of Acylcarnitines in Complex Mixtures. *Anal. Chem.* **2002**, *74*, 5799–5806.
204. van der Hooft, J.J.J.; Ridder, L.; Barrett, M.P.; Burgess, K.E. V Enhanced Acylcarnitine Annotation in High-Resolution Mass Spectrometry Data: Fragmentation Analysis for the Classification and Annotation of Acylcarnitines . *Front. Bioeng. Biotechnol.* 2015, *3*.
205. Evans, E.H.; Pisonero, J.; Smith, C.M.M.; Taylor, R.N. Atomic Spectrometry Update: Review of Advances in Atomic Spectrometry and Related Techniques. *J. Anal. At. Spectrom.* **2020**, *35*, 830–851.
206. Agüi-Gonzalez, P.; Jähne, S.; Phan, N.T.N. SIMS Imaging in Neurobiology and Cell Biology. *J. Anal. At. Spectrom.* **2019**, *34*, 1355–1368.
207. Hartnell, D.; Andrews, W.; Smith, N.; Jiang, H.; McAllum, E.; Rajan, R.; Colbourne, F.; Fitzgerald, M.; Lam, V.; Takechi, R.; et al. A Review of Ex Vivo Elemental Mapping Methods to Directly Image Changes in the Homeostasis of Diffusible Ions (Na+, K+, Mg2 +, Ca2 +, Cl–) Within Brain Tissue. *Front. Neurosci.* **2020**, *13*, 1–8.
208. de Jesus, J.M.; Costa, C.; Burton, A.; Palitsin, V.; Webb, R.; Taylor, A.; Nikula, C.; Dexter, A.; Kaya, F.; Chambers, M.; et al. Correlative Imaging of Trace Elements and Intact Molecular Species in a Single-Tissue Sample at the 50 Mm Scale. *Anal. Chem.* **2021**, *93*, 13450–13458.
209. Liu, H.; Chen, R.; Wang, J.; Chen, S.; Xiong, C.; Wang, J.; Hou, J.; He, Q.; Zhang, N.; Nie, Z.; et al. 1,5-Diaminonaphthalene Hydrochloride Assisted Laser Desorption/Ionization Mass Spectrometry Imaging of Small Molecules in Tissues Following Focal Cerebral Ischemia. *Anal. Chem.* **2014**, *86*, 10114–10121.
210. Chehardoli, G.; Bahmani, A. The Role of Crown Ethers in Drug Delivery. *Supramol. Chem.* **2019**, *31*, 221–238.
211. Izatt, R.M.; Bradshaw, J.S.; Nielsen, S.A.; Lamb, J.D.; Christensen, J.J.; Sen, D. Thermodynamic and Kinetic Data for Cation-Macrocycle Interaction. *Chem. Rev.* **1985**, *85*, 271–339.

212. Gokel, M.R.; McKeever, M.; Meisel, J.W.; Negin, S.; Patel, M.B.; Yin, S.; Gokel, G.W. Crown Ethers Having Side Arms: A Diverse and Versatile Supramolecular Chemistry. *J. Coord. Chem.* **2021**, *74*, 14–39.
213. Calder, P.C. Eicosanoids. *Essays Biochem.* **2020**, *64*, 423–441.
214. Fujino, H. Why PGD2 Has Different Functions from PGE2. *BioEssays* **2021**, *43*, 2000213.
215. Jansson, E.T. Strategies for Analysis of Isomeric Peptides. *J. Sep. Sci.* **2018**, *41*, 385–397.
216. Mesa Sanchez, D.; Creger, S.; Singla, V.; Kurulugama, R.T.; Fjeldsted, J.; Laskin, J. Ion Mobility-Mass Spectrometry Imaging Workflow. *J. Am. Soc. Mass Spectrom.* **2020**, *31*, 2437–2442.
217. Sans, M.; Feider, C.L.; Eberlin, L.S. Advances in Mass Spectrometry Imaging Coupled to Ion Mobility Spectrometry for Enhanced Imaging of Biological Tissues. *Curr. Opin. Chem. Biol.* **2018**, *42*, 138–146.
218. McLean, J.A.; Ridenour, W.B.; Caprioli, R.M. Profiling and Imaging of Tissues by Imaging Ion Mobility-Mass Spectrometry. *J. Mass Spectrom.* **2007**, *42*, 1099–1105.
219. Paglia, G.; Kliman, M.; Claude, E.; Geromanos, S.; Astarita, G. Applications of Ion-Mobility Mass Spectrometry for Lipid Analysis. *Anal. Bioanal. Chem.* **2015**, *407*, 4995–5007.
220. Michael, J.A.; Mutuku, S.M.; Ucur, B.; Sarretto, T.; Maccarone, A.T.; Niehaus, M.; Trevitt, A.J.; Ellis, S.R. Mass Spectrometry Imaging of Lipids Using MALDI Coupled with Plasma-Based Post-Ionization on a Trapped Ion Mobility Mass Spectrometer. *Anal. Chem.* **2022**, *94*, 17494–17503.
221. Crotti, S.; Menicatti, M.; Pallecchi, M.; Bartolucci, G. Tandem Mass Spectrometry Approaches for Recognition of Isomeric Compounds Mixtures. *Mass Spectrom. Rev.* **2023**, *42*, 1244–1260.
222. Cao, H.; Xiao, L.; Park, G.; Wang, X.; Azim, A.C.; Christman, J.W.; van Breemen, R.B. An Improved LC-MS/MS Method for the Quantification of Prostaglandins E(2) and D(2) Production in Biological Fluids. *Anal. Biochem.* **2008**, *372*, 41–51.
223. Schmidt, L.; Burmeister, L.S.; Greinacher, A.; König, S.; Garscha, U. Development of SFC-MS Method for Quantification of Eicosanoids Biosynthesized in Primary Human Blood Cells. *Metabolites* 2022, *12*.
224. Kumari A. Ubhayasekera, S.J.; Acharya, S.R.; Bergquist, J. A Novel, Fast and Sensitive Supercritical Fluid Chromatography-Tandem Mass Spectrometry (SFC-MS/MS) Method for Analysis of Arachidonic Acid Metabolites. *Analyst* **2018**, *143*, 3661–3669.
225. Murphy, R.C.; Barkley, R.M.; Zemski Berry, K.; Hankin, J.; Harrison, K.; Johnson, C.; Krank, J.; McAnoy, A.; Uhlson, C.; Zarini, S. Electrospray Ionization and Tandem Mass Spectrometry of Eicosanoids. *Anal. Biochem.* **2005**, *346*, 1–42.
226. Schmidt, R.; Coste, O.; Geisslinger, G. LC-MS/MS-Analysis of Prostaglandin E2 and D2 in Microdialysis Samples of Rats. *J. Chromatogr. B, Anal. Technol. Biomed. life Sci.* **2005**, *826*, 188–197.
227. Wu, H.-T.; Riggs, D.L.; Lyon, Y.A.; Julian, R.R. Statistical Framework for Identifying Differences in Similar Mass Spectra: Expanding Possibilities for Isomer Identification. *Anal. Chem.* **2023**, *95*, 6996–7005.
228. Borràs, E.; Pastor, O.; Sabidó, E. Use of Linear Ion Traps in Data-Independent Acquisition Methods Benefits Low-Input Proteomics. *Anal. Chem.* **2021**, *93*, 11649–11653.

229. Wu, Q.; Li, Y.; Wang, Y.; Lu, H. Quantitative Mass Spectrometry Imaging of Amino Acids with Isomer Differentiation in Brain Tissue via Exhaustive Liquid Microjunction Surface Sampling–Tandem Mass Tags Labeling–Ultra Performance Liquid Chromatography–Mass Spectrometry. *J. Chromatogr. A* **2020**, *1621*, 461086.
230. Duncan, K.D.; Lanekoff, I. Oversampling to Improve Spatial Resolution for Liquid Extraction Mass Spectrometry Imaging. *Anal. Chem.* **2018**, *90*, 2451–2455.
231. Ferguson, L.; Bradshaw, R.; Wolstenholme, R.; Clench, M.; Francese, S. Two-Step Matrix Application for the Enhancement and Imaging of Latent Fingermarks. *Anal. Chem.* **2011**, *83*, 5585–5591.
232. Huang, J.; Gao, S.; Wang, K.; Zhang, J.; Pang, X.; Shi, J.; He, J. Design and Characterizing of Robust Probes for Enhanced Mass Spectrometry Imaging and Spatially Resolved Metabolomics. *Chinese Chem. Lett.* **2023**, *34*, 107865.
233. Esteve, C.; Tolner, E.A.; Shyti, R.; van den Maagdenberg, A.M.J.M.; McDonnell, L.A. Mass Spectrometry Imaging of Amino Neurotransmitters: A Comparison of Derivatization Methods and Application in Mouse Brain Tissue. *Metabolomics* **2016**, *12*, 30.
234. O'Neill, K.C.; Lee, Y.J. Visualizing Genotypic and Developmental Differences of Free Amino Acids in Maize Roots With Mass Spectrometry Imaging . *Front. Plant Sci.* 2020, *11*.
235. Wang, X.; Hou, Y.; Hou, Z.; Xiong, W.; Huang, G. Mass Spectrometry Imaging of Brain Cholesterol and Metabolites with Trifluoroacetic Acid-Enhanced Desorption Electrospray Ionization. *Anal. Chem.* **2019**, *91*, 2719–2726.

Acta Universitatis Upsaliensis

Digital Comprehensive Summaries of Uppsala Dissertations from the Faculty of Science and Technology 2307

Editor: The Dean of the Faculty of Science and Technology

A doctoral dissertation from the Faculty of Science and Technology, Uppsala University, is usually a summary of a number of papers. A few copies of the complete dissertation are kept at major Swedish research libraries, while the summary alone is distributed internationally through the series Digital Comprehensive Summaries of Uppsala Dissertations from the Faculty of Science and Technology. (Prior to January, 2005, the series was published under the title "Comprehensive Summaries of Uppsala Dissertations from the Faculty of Science and Technology".)

Distribution: publications.uu.se
urn:nbn:se:uu:diva-511811

ACTA UNIVERSITATIS
UPSALIENSIS
2023